Spring 5-15-2019

Solid-state NMR Study on Solid Amine Sorbents

Chia-Hsin Chen
Washington University in St. Louis

WASHINGTON UNIVERSITY IN ST. LOUIS

Department of Chemistry

Dissertation Examination Committee:

Sophia Hayes, Chair

Alexander Barnes

Jonathan Barnes

Julio D'Arcy

Daniel Giammar

Solid-state NMR Study on Solid Amine Sorbents

by

Chia-Hsin Chen

A dissertation presented to
The Graduate School
of Washington University in
partial fulfillment of the
requirements for the degree
of Doctor of Philosophy

May 2019

St. Louis, Missouri

Table of Contents

List of Figures

List of Tables

Acknowledgments

I thank the co-funded fellowship by Taiwan Ministry of Education and Washington University for supporting me for four years. The research work is mainly supported by two funding and they are gratefully acknowledged. One funding is from the National Science Foundation (CBET-1403298 and CBET-1403239). The other is the Center for Understanding and Control of Acid Gas-Induced Evolution of Materials for Energy (UNCAGE-ME), an Energy Frontier Research Center funded by U.S. Department of Energy (US DOE), Office of Science, Basic Energy Sciences (BES) under Award No. DESC0012577. I thank Dr. Christopher Jones, Dr. Carsten Sievers and the graduate student Jason Lee for the excellent collaboration and many fruitful discussions. I thank Dr. Alexander Barnes and Dr. Erika Sesti for running DNP and low temperature MAS and always inspiring ideas. I thank Dr. Frederic Mentink-Vigier in National High Magnetic Field Lab (NHMFL) for running the low temperature NMR and provide many suggestions. I thank Prof. Anne Lesage, Dr. David Gajan, and Dr. Dorothea Wisser, CNRS for performing DNP NMR and for their many suggestions to data analysis. I thank Dr. Johannes E. Leisen at the Georgia Institute of Technology NMR Center, and Dr. Tanya L. Whitmer in NMR Laboratory in the Department of Chemistry, The Ohio State University NMR Facility for acquisition of low temperature MAS NMR experiments. I thank the training of the Department of Chemistry, Washington University, and the great amount of support from the staff in the department. I thank my defense committee: Dr. Alexander Barnes, Dr. Julio D'Arcy, Dr. Jonathan Barnes, and Dr. Daniel Giammar for giving me valuable advice on oral presentation and dissertation thesis.

As an international student, it is challenging to study for a doctoral degree. Without the help from many kind people, I can not make this far. I am lucky to be in the Hayes group because every group member is very kind and willing to help me not only in academic pursuits but also in daily life. The reason why the Hayes group is so warm and funny is because the amazing group leader, Dr. Sophia Hayes. Sophia is a very kind, warm and intelligent advisor. I appreciate the opportunity to conduct my graduate research under her guidance. I thank her for all the training and many life-time opportunities such as research trips to CNRS, Lyon in France, OSU and Georgia Tech. I also want to thank Sophia for not limiting me in research directions and allowing me to try many crazy ideas. Zayd was very supportive and very patient teaching me NMR knowledge. Katie helped me with the experimental setup when I started in the lab, and showed me how to design the experiments. I enjoyed my time working with Erika and thank her for editing my thesis. Blake was very helpful when I started a training project. He taught me literature research, experimental setup and data processing. I also learned about the Midwest farmer culture which is very interesting. Although Matt and I are in very different research project, Matt is an intelligent person and I enjoyed our NMR discussions. Robert is the kindest and most humble person I have ever known. I am so lucky to have him as my co-worker and learn so much from him. I am glad that we are in the same year and learned together. Daphna and I work together in the same research project. We got to know each other, and it is interesting that with different culture background, we have many interests in common. I enjoyed working with Daphna and learned to be resourceful in research. I thank Ike for doing the lab business together and many NMR discussions. I also want to thank other group members, Yvonne, Jinlei and Jason for the help over years.

I would also want to thank a group of people who are from Taiwan: Amanda, Nai-Wen, Yi-ling, Paul, Bear's family, Ching-Ying, Nai-Hua, Yung-Ching, Wen-Chich and many others. They have similar experience of studying and living in STL, and have shared their experience to encourage and help me since I arrived. I am proud that I am from Taiwan and know these awesome and passionate people.

The last and most important thanks are to my parents. I am not a good student by paper, but they always believe in me and encourage me to do and try things I am interested about. They love me very much and always save the best things for me. Without their support and guidance, I could not have found my passion and pursued it.

Chia-Hsin Chen

Washington University in St. Louis

May 2019

Dedicated to my parents, Chung-Ho Chen and Yu-Feng Lin

ABSTRACT OF THE DISSERTATION

Solid-NMR study on solid amine sorbents

for Arts & Sciences Graduate Students

by

Chia-Hsin Chen

Doctor of Philosophy in Chemistry

Washington University in St. Louis, 2019

Professor Sophia Hayes, Chair

Solid-state NMR spectroscopy is a useful structural tool, with a high sensitivity to the local atomic-scale environment providing a powerful probe of structure, disorder, and dynamics of solids. In this dissertation, solid-state NMR was used to characterize chemisorbed products of solid amine sorbents exposed to CO_2. Solid amine sorbents are promising candidates to capture CO_2 for the purposes of mitigation of this greenhouse gas in high-concentration sources, such as flue gases emitted from power plants or industrial sites. Understanding the adsorption process of these solid materials is critical to help design better materials to have a higher CO_2 uptake.

A series of solid-state NMR methods were employed to study these materials. ^{15}N CPMAS of primary amines (APS) before and after $^{13}CO_2$ was employed, and the result is informative. With the time-evolution of signals before and after CO_2 exposure, the decreased intensity of the reactant resonance and increased intensity of the products' resonances, we were able to assign amine, ammonium, and carbamate in ^{15}N spectra. Complementary $^{13}C\{^{15}N\}$ REDOR and $^{15}N\{^{13}C\}$ REDOR of a primary amine (APS) were used to obtain the ^{13}C-^{15}N dipolar interaction of the chemisorbed product species corresponding the distances of both directly-bonded C-N of

carbamate and the distant interaction between of carbamate to its ammonium counter ion that is ion-paired to it.

Under humid (or damp) conditions, hydrated bicarbonate was found in three types of amine: primary, secondary, and tertiary. NMR measurements show the hydrated bicarbonate undergoes dynamic motion at room temperature induced by surrounding water. Different water environments lead to chemically-inequivalent bicarbonates, which results in two ^{13}C signals when bicarbonate is cooled down (100 K). Exposure to D_2O, replacing water, allowed for interactions between the two bicarbonate species and the surrounding environments to be elucidated, via low-temperature ^{13}C-^{1}H HETCOR.

Additionally, dynamic nuclear polarization (DNP) NMR was successfully performed on primary amines (APS). 2D DNP HETCOR was used to determine the interactions between carbamate pendant molecules and the surrounding environment. ^{13}C-^{1}H HETCOR, ^{15}N-^{1}H HETCOR, and ^{29}Si-^{1}H HETCOR (all using enhancements provided by DNP) were performed, and the results show coupling between carbamate and the hydroxyl groups on the SBA15 (silica) surface.

Chapter 1: Introduction

1.1 Solid-state NMR

Solid-state nuclear magnetic resonance (NMR) spectroscopy is a powerful analytical technique that exploits the interactions they experience with surrounding atoms and electrons to provide atomic-level information of the structure of solids. NMR signals are the responses of samples to radio frequency (RF) irradiation in an external magnetic field, and can be described by several interactions including RF pulses, spin properties, and interactions between spins. The total Hamiltonian is in Equation 1.1.[1,2]

$$\hat{H} = \hat{H}_z + \hat{H}_{RF} + \hat{H}_J + \hat{H}_{CS} + \hat{H}_D + \hat{H}_Q \qquad \text{Equation 1.1}$$

$\hat{H}_z$ is Zeeman Hamiltonian which is typically the dominant interaction, and represents the interaction between the spins of the sample to the external magnetic field. $\hat{H}_{RF}$ is the term to address the interaction of spins to applied radio frequencies. $\hat{H}_J, \hat{H}_{CS}, \hat{H}_D \; and \; \hat{H}_Q$ are the four internal Hamiltonians which can each lead to a broadening of NMR spectra. However, these four Hamiltonians interactions which are often anisotropic and can provide chemical information, especially structural and conformational information. $\hat{H}_J$ is scalar coupling of two nuclei through bonding electrons, and the magnitude is usually less than 100 Hz so typically unresolved in solid-state NMR. $\hat{H}_{CS}$ represents the chemical shift interaction, and this Hamiltonian describes the shielding effects of electrons around the nuclei. $\hat{H}_D$ is the dipole-dipole coupling describing the interaction between two spins through space. $\hat{H}_Q$ is the quadrupolar Hamiltonian for the nuclei with nuclear spin quantum numbers (I) $>\frac{1}{2}$ which describes the interaction with the electric field gradient (EFG) at a nucleus.[3]

1.2 Solid-state NMR methods

Solid-state NMR spectra are broadened by a range of anisotropic interactions,[1,2] and several advanced NMR techniques are required to improve resolution and sensitivity before structural information can be extracted. In this dissertation, we focus on the spin-$\frac{1}{2}$ nuclei, ^{1}H, ^{13}C, ^{15}N and ^{29}Si, so $\widehat{H}_Q$ will not be discussed. The methods that were employed to reduce the broadening from $\widehat{H}_{CS}$ and $\widehat{H}_D$ are briefly introduced below:

Magic-angle spinning (MAS): MAS is used routinely to provide high-resolution NMR spectra of solids by removing the effects of chemical shift anisotropy and dipolar interactions. Both $\widehat{H}_{CS}, and\ \widehat{H}_D$ share a term of ($3cos^2\theta - 1$)[1,2] in their Hamiltonians, so if the sample is spun rapidly at the angle of 54.74° with respect the external magnetic field, the anisotropic broadening effects will be patially averaged, leading to a sharp isotropic peak.[1,2] We employ spinning from ≈ 5 kHz to 25 kHz, and MAS probes can spin as high as the frequency as ≈ 100 kHz.[4]

Cross-polarization magic-angle spinning (CPMAS): CPMAS is commonly used in solid-state NMR especially for the low natural abundance nuclei such as ^{13}C (1.1%), ^{29}Si (4.6 %) and ^{15}N (0.3%) to enhance the NMR signal. There are two major drawbacks to acquire these low abundance nuclei NMR: one is their inherently low sensitivity by being both low in abundance and low gyromagnetic ratio, γ. Another drawback is that all 3 nuclear spins typically have long possess long relaxation time (T_1). CPMAS uses the inherently higher polarization from abundant nuclei, such as ^{1}H, and transfer that polarization to the low-abundance nuclei.[5,6] CPMAS also allows the low-abundance nuclei to relax at the rate of the faster ^{1}H relaxation, so enhanced NMR signals from the ^{1}H polarization, and more rapid T_1 times shorten the time to acquire good signals. CPMAS experiments rely on the heteronuclear dipolar interaction, meaning this technique is unable to detect isolated nuclei, making CPMAS inherently not quantitative without

additional calibration steps. Additionally, CPMAS does not work with the dynamic species because of the dipole-dipole interaction averaging to zero.

Correlation spectra (HETCOR): The interactions between the different types of nuclear spins can provide information on their through-bond connectivity and through-space proximity and can be measured by two-dimensional homonuclear or heteronuclear correlation spectra.[2,7,8]

1.3 Characterization of chemisorbed products of CO_2 capture materials

Fossil fuel combustion creates a large amount of atmospheric CO_2.[9] High concentrations of CO_2 are believed to be a major contributor to global climate change, causing a negative on our environment and society.[10] The aim of mitigating global climate change prompts the research of carbon capture and storage (CCS). The goal of CCS is to reduce CO_2 emission to atmosphere by capturing CO_2, from large CO_2 emitters such as that found in the flue gas of power plants, and store the CO_2 by geosequestration underground.[11,12] Aqueous amine solutions are the current technology used to capture CO_2 in some power plants.[13] However, these amine solutions are inefficient in sample regeneration (meaning requiring a large input of energy to release the adsorbed CO_2), leading to high costs. Solid amine sorbents materials have lower regeneration energy and are less corrosive to the equipment, therefore is a promising material to replace the current aqueous amine technologies.[14,15] Amine-tethered mesoporous silica has a large surface area and is easy to modify with different functional groups to have a high CO_2 uptake.[14,15] Unlike aqueous amines, which have been extensively studied[16], the mechanism of CO_2 adsorption in solid amine adsorbents is still ambiguous.[14,17,18] The mechanism of CO_2 interactions with solid amine adsorbents was assumed to be similar to the aqueous amines and to form carbamic acid, carbamate, and bicarbonate which are shown in Scheme 1.1. In solid amines, there are several

parameters that influence the formation of the chemisorbed products such as humidity, the type of amine, partial pressure of CO_2, and the sample preparation before CO_2 loading. It is challenging to characterize amorphous systems such as mesoporous silica with common characterization techniques such as X-ray diffraction because of the lack of long-range order. There are studies using Fourier transform IR (FTIR) to identify products[19–23], however, the important C=O, NH_3^+, and COO^- vibrational bands have similar frequencies leading to overlap and the difficulty for interpretation. Solid-state NMR is a powerful tool to characterize chemical structure at the atomic level and to quantify chemical components, not limited by amorphous or, with the proper approach, overlapping resonances.

Several groups observed different chemisorbed products in solid amine sorbents other than the proposed chemisorbed products in Scheme 1.1– carbamic acid, carbamate and bicarbonate. Danon et al. used FTIR spectra for different densities of primary amines on SBA15 and observed two types of carbamate, ammonium carbamate and silylpropylcarbamate (also known as "surface-bound carbamate" for the latter) for a low density of amines on SBA.[19] High-density amines on SBA15, in contrast, showed only ammonium carbamate.[24] Our group reported (Moore et al. [25]) used solid-state NMR on hyperbranched amine polymers on SBA15 and observed multiple chemisorbed species. We observed two T_2 relaxation times for a ^{13}C resonance in the region typically assigned to carbamate, and concluded this resonance was therefore composed another type of carbamate or bicarbonate. Foo et al. used in-situ FTIR to investigate a study on three different amines-- primary, secondary and tertiary-- on SBA15. They suggest that a secondary amine could form two types of carbamic acid: a monomer and a dimer.[20] Forse et al. used solid-state NMR and DFT calculations on a similar solid amine material, a metal organic framework with amine linkers, Zn_2 (dobpdc), and assigned the ^{13}C 161 ppm resonance to the

carbamic acid dimer.[26] The ^{13}C 161 ppm resonance is the first solid-state NMR evidence showing a distinguishable carbamic acid dimer. Mafra et al observed a new chemisorbed species at ^{13}C 153 ppm and assigned it to a different type of carbamic acid. This carbamic acid is believed to be sensitive to moisture and only exists at extremely dry conditions.[27]

Although many groups have attempted to use FTIR and solid-state NMR to identify the chemisorbed products of similar solid amine systems, the inconsistent results reflect the complexity of the chemical environment and the resulting spectra, which are difficult to interpret. In this dissertation, we used the consistent set of experimental conditions including sample activation, density of amine groups on SBA15, and CO_2 exposure time. We observed that the chemisorbed species have considerable variability depending on these conditions, and even such chemisorbed products tended to revert to CO_2 and reactant amines and desorb under ambient temperature and pressure.

1.4 Synthesis of amine-SBA15

To synthesize SBA15, Pluronic P-123 (24.0 g) was dissolved in concentrated HCl (120 mL) and distilled water (636 mL) in a 2 L Erlenmeyer flask. The solution was then stirred for 3 h at room temperature. Afterwards, tetraethyl orthosilicate (46.24 g) was added dropwise to the solution. The solution was then stirred continuously for 20 h at 40 °C. The mixture was then quenched and filtered with excess distilled water. The resulting white powder was then dried in an oven overnight at 75 °C. Afterwards, the sample was put into a calcination oven. To calcine the white powder, it was heated to 200 °C at 1.0 °C min−1, held at that temperature for 2 h, heated to 550 °C at 1.0 °C min−1, held at that temperature for 6 h, and finally cooled to room temperature.

To graft 3-aminopropyltrimethoxysilane, SBA15 was evacuated on a Schlenk line at 120 °C at a pressure of <20 mTorr overnight. Approximately 2 g of SBA15 was added to a flask with 200 mL

of toluene. Next, the aminosilane (APS, MAPS, and DMAPS) was added to the solution and stirred at 85 °C for 24 h. The resulting product was then filtered with toluene, hexane, and ethanol and evacuated on the Schlenk line at 120 °C and at a pressure of <20 mTorr overnight. The physical properties are derived from nitrogen physisorption and nitrogen content of the resulting products (Table 1.1).

Adsorbent	Surface area (m^2g^{-1})	Pore volume (cm^3g^{-1})	N content ($mmolNg^{-1}$)
SBA15	950	0.96	-
APS-SBA15	433	0.56	2.4
MAPS-SBA15	371	0.49	2.5
DMAPS-SBA15	418	0.52	2.1

Table 1.1 physical properties derived from nitrogen physisorption and nitrogen content adsorbents.

1.5 Synthesis of [^{15}N] APS-SBA15

Prior to 3-bromopropylsilane grafting, SBA15 was dried overnight under a pressure of <20 mTorr at 120 °C on a Schlenk line. Approximately 10 mL of toluene per gram of SBA15 and 1.2 mL of distilled water per gram SBA15 were then added to a pressure tube, and everything was stirred for 2 h at room temperature. (3-bromopropyl)-trimethoxysilane was then added to the solution, and the sample was heated to 120 °C and stirred for 24 h. The reaction mixture was then filtered and washed with copious amounts of toluene, hexane, and ethanol. Subsequently, the sample was put on a Schlenk line and dried overnight at a pressure of <20 mTorr at 120 °C.

The amination of the 3-bromopropylsilane grafted SBA15 was performed in a 50 mL Parr reactor equipped with a temperature controller, a J-type thermocouple, a 3000 psi rupture disk, and a pressure gauge. The procedure was similar to that reported previously.[16] The stainless steel tubing plumbed to the reactor was 0.125 inch in diameter and a three way ball valve was used to direct ammonia or helium to the Parr reactor. A Teflon cylinder that had six evenly spaced holes drilled into it was used as a sample holder.

The sample holder also had an internal screw such that samples could be sealed with a frit under high pressure. The Parr reactor was kept in a drying oven (100 °C) prior to each use. All reactions were done in a fume hood. Before each reaction, the empty Parr reactor was further dried by flowing helium at 100 °C for 2 h. The 3-bromopropylsilane grafted SBA15 was then loaded into the Teflon cylinder and then sealed with a 0.5 in stainless steel porous disk (2 μm). The disk allowed ammonia to permeate the sample holder while preventing the powder sample from dispersing during pressure changes. The sealed sample holder was then put into the cup of the Parr reactor, which was then fitted and sealed with a Teflon o-ring. A leak test was then performed by pressurizing the reactor with 1000 psi of helium. After a successful leak test, all the helium in the reactor was released. Next, $^{15}NH_3$ was introduced into the reactor with the outlet valve closed. To condense as much labeled ammonia into the reactor as possible, the cup of the reactor was immersed into a Dewar filled with liquid nitrogen. After the temperature of the reactor reached -60 °C, the inlet valve was shut, and the reactor cup was warmed up to room temperature. While keeping the inlet and outlet valves closed, the reactor was then heated to 100 °C for 5 h. After the reaction, ammonia was released into a beaker filled with water. The reactor was further purged with helium for 15 min. The reaction product was then filtered and washed with copious amounts of aqueous ammonia and dried overnight on a Schlenk line under a pressure of <20 mTorr and at a temperature of 120 °C. This sample is named [^{15}N] APS-SBA. The sample was sent to Atlantic Microlabs (Norcross, GA, USA) for elemental analysis to ensure that no bromine was left on the sample. The amine loading of [^{15}N] APS- SBA is 1.5 mmol N/g.

1.6 Overview of chapters

There are four chapters of this dissertation. Chapter 1 is an introduction of solid-state NMR and a literature review of solid-state NMR of CO_2 chemisorbed product species on solid-amine SBA15. Chapter 2 is describes a series of NMR methods to determine the chemisorbed products species of solid-amine SBA15. A Combination of $^{13}C\{^{15}N\}$ REDOR and $^{15}N\{^{13}C\}$ REDOR were performed on a primary amine, and the results shows the chemisorbed products comprised carbamic acid, carbamate and possibly bicarbonate. We monitored the desorption process of a primary amine and found that carbamic acid is the first species to desorb. In chapter 3, we study the chemisorbed product species under humid (damp) conditions. Hydrated bicarbonate is found in all three amines: primary, secondary, and tertiary. The hydrated bicarbonate splits into two ^{13}C signals at 100 K. We replaced water with D_2O to examine the two ^{13}C signals of bicarbonate, and the results suggest that different water environments cause chemically and magnetically inequivalent sites. In chapter 4, we performed DNP NMR on solid-amine SBA15, and the DNP enhancement enables the 2D correlation spectra. The ^{13}C-^{1}H HETCOR, ^{15}N-^{1}H HETCOR, and ^{29}Si-^{1}H HETCOR data reveal the conformation of the chemisorbed products– carbamate ion pair is coupled to the SBA surface.

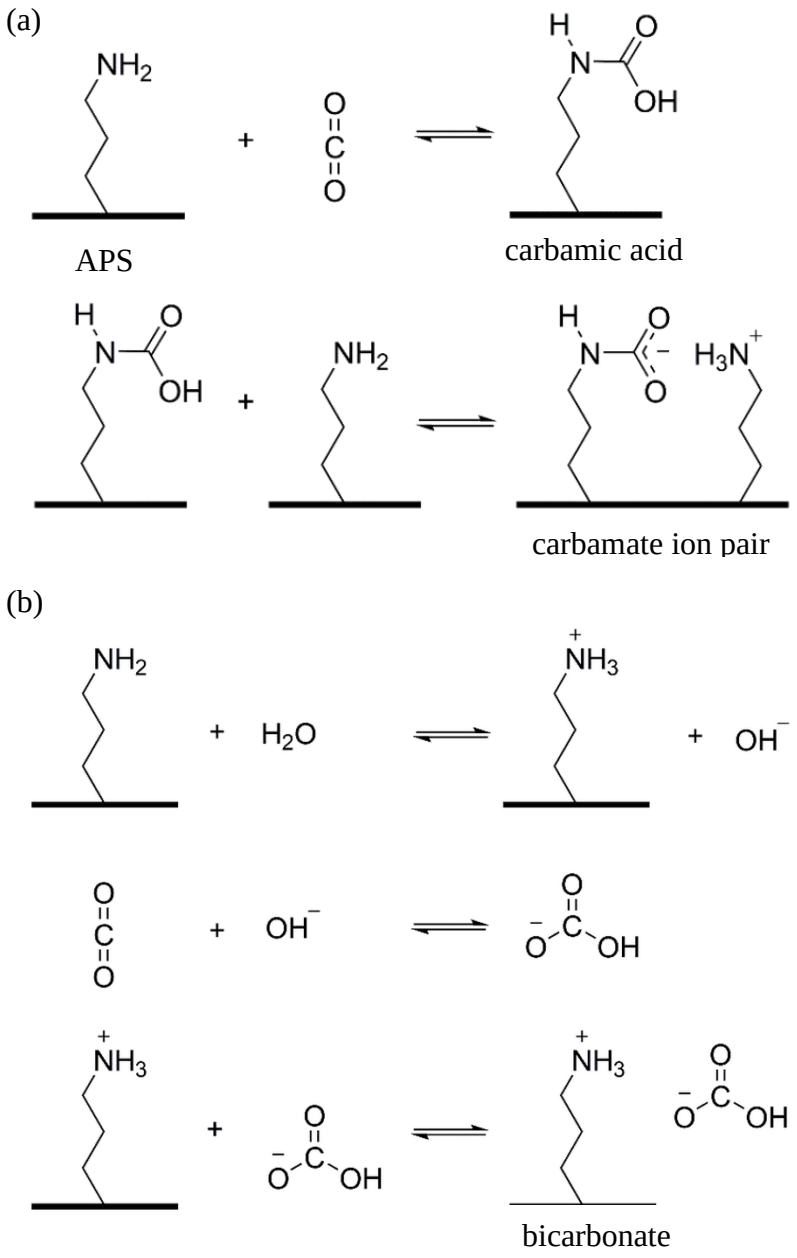

Scheme 1.1 (a) hypothesized fomation of carbamic acid and subsequent carbamate formation. (b) hypothesized fomation of bicarbonate (when H_2O is present). Note: both result in one pendant amine forming an ammonium cation.

References (Chapter 1)

(1) Duer, M. J. *Solid-State NMR Spectroscopy Principles and Applications*; Duer, M. J., Ed.; Blackwell Science Ltd: Oxford, UK, 2001.

(2) Apperley, D. C.; Harris, R. K. (Robin K.; Hodgkinson, P. *Solid-State NMR : Basic Principles & Practice*; Momentum Press, 2012.

(3) Wasylishen, R. E.; Ashbrook, S. E.; Wimperis, S. *NMR of Quadrupolar Nuclei in Solid Materials*; John Wiley & Sons, Ltd: Chichester, UK, 2012.

(4) Penzel, S.; Smith, A. A.; Agarwal, V.; Hunkeler, A.; Org, M.-L.; Samoson, A.; Böckmann, A.; Ernst, M.; Meier, B. H. Protein Resonance Assignment at MAS Frequencies Approaching 100 KHz: A Quantitative Comparison of J-Coupling and Dipolar-Coupling-Based Transfer Methods. *J. Biomol. NMR* **2015**, *63* (2), 165–186.

(5) Fyfe, C. A.; Brouwer, D. H.; Tekely, P. Measurement of NMR Cross-Polarization (CP) Rate Constants in the Slow CP Regime: Relevance to Structure Determinations of Zeolite-Sorbate and Other Complexes by CP Magic-Angle Spinning NMR. *J. Phys. Chem. A* **2005**, *109*, 6187–6192.

(6) Stejskal, E. O.; Schaefer, J.; Waugh, J. S. Magic-Angle Spinning and Polarization Transfer in Proton-Enhanced NMR. *J. Magn. Reson.* **1977**, *28*, 105–112.

(7) Sangodkar, R. P.; Smith, B. J.; Gajan, D.; Rossini, A. J.; Roberts, L. R.; Funkhouser, G. P.; Lesage, A.; Emsley, L.; Chmelka, B. F. Influences of Dilute Organic Adsorbates on the Hydration of Low-Surface-Area Silicates. *J. Am. Chem. Soc.* **2015**, *137*, 8096–8112.

(8) Amoureux, J. P.; Trébosc, J.; Delevoye, L.; Lafon, O.; Hu, B.; Wang, Q. Correlation

NMR Spectroscopy Involving Quadrupolar Nuclei. *Solid State Nucl. Magn. Reson.* **2009**, *35*, 12–18.

(9) Olivier, J. G. J.; PBL Netherlands Environmental Assessment Agency. *Trends in Global CO_2 Emissions 2013 Report*; PBL Netherlands Environmental Assessment Agency, 2013.

(10) Cramer, W.; Bondeau, A.; Woodward, F. I.; Prentice, I. C.; Betts, R. A.; Brovkin, V.; Cox, P. M.; Fisher, V.; Foley, J. A.; Friend, A. D.; et al. Global Response of Terrestrial Ecosystem Structure and Function to CO_2 and Climate Change: Results from Six Dynamic Global Vegetation Models. *Glob. Chang. Biol.* **2001**, *7*, 357–373.

(11) Samanta, A.; Zhao, A.; Shimizu, G. K. H.; Sarkar, P.; Gupta, R. Post-Combustion CO_2 Capture Using Solid Sorbents: A Review. *Ind. Eng. Chem. Res* **2012**, *51*, 1438–1463.

(12) Sayari, A.; Belmabkhout, Y.; Da'na, E. CO_2 Deactivation of Supported Amines: Does the Nature of Amine Matter? *Langmuir* **2012**, *28*, 4241–4247.

(13) and, A. B. R.; Rubin*, E. S. A Technical, Economic, and Environmental Assessment of Amine-Based CO2 Capture Technology for Power Plant Greenhouse Gas Control. *Environ. Sci. Technol.* **2002**, *36*, 4467–4475.

(14) Didas, S. A.; Choi, S.; Chaikittisilp, W.; Jones, C. W. Amine–Oxide Hybrid Materials for CO_2 Capture from Ambient Air. *Acc. Chem. Res.* **2015**, *48*, 2680–2687.

(15) Hahn, M. W.; Jelic, J.; Berger, E.; Reuter, K.; Jentys, A.; Lercher, J. A. Role of Amine Functionality for CO_2 Chemisorption on Silica. *J. Phys. Chem. B* **2016**, *120*, 1988–1995.

(16) Kortunov, P. V.; Siskin, M.; Baugh, L. S.; Calabro, D. C. In Situ Nmr Mechanistic Studies

of Carbon Dioxide Reactions With Liquid Amines in Aqueous Systems: New Insights on Carbon Capture Reaction Pathways. *Energy & Fuels* **2015**, *29*, 5919–5939.

(17) Bollini, P.; Didas, S. A.; Jones, C. W. Amine-Oxide Hybrid Materials for Acid Gas Separations. *J. Mater. Chem.* **2011**, *21*, 15100–15120.

(18) Didas, S. A.; Kulkarni, A. R.; Sholl, D. S.; Jones, C. W. Role of Amine Structure on Carbon Dioxide Adsorption from Ultradilute Gas Streams Such as Ambient Air. **2012**, 2058–2064.

(19) Danon, A.; Stair, P. C.; Weitz, E. FTIR Study of CO_2 Adsorption on Amine Grafted SBA-15 : Elucidation of Adsorbed Species. *J. Phys. Chem. C* **2011**, *115*, 11540–11549.

(20) Foo, G. S.; Lee, J. J.; Chen, C.-H.; Hayes, S. E.; Sievers, C.; Jones, C. W. Elucidation of Surface Species through in Situ FTIR Spectroscopy of Carbon Dioxide Adsorption on Amine-Grafted SBA-15. *ChemSusChem* **2016**, *9*, 1–12.

(21) Knöfel, C.; Martin, C.; Hornebecq, V.; Llewellyn, P. L. Study of Carbon Dioxide Adsorption on Mesoporous Aminopropylsilane-Functionalized Silica and Titania Combining Microcalorimetry and in Situ Infrared Spectroscopy. *J. Phys. Chem. C* **2009**, *113*, 21726–21734.

(22) Bacsik, Z.; Ahlsten, N.; Ziadi, A.; Zhao, G. Y.; Garcia-Bennett, A. E.; Martín-Matute, B.; Hedin, N. Mechanisms and Kinetics for Sorption of CO_2 on Bicontinuous Mesoporous Silica Modified with n-Propylamine. *Langmuir* **2011**, *27*, 11118–11128.

(23) Lee, J. J.; Chen, C.-H.; Shimon, D.; Hayes, S. E.; Sievers, C.; Jones, C. W. Effect of Humidity on the CO_2 Adsorption of Tertiary Amine Grafted SBA-15. *J. Phys. Chem. C*

2017, *121*, 23480–23487.

(24) Didas, S. A.; Sakwa-novak, M. A.; Foo, G. S.; Sievers, C.; Jones, C. W. Effect of Amine Surface Coverage on the Co-Adsorption of CO_2 and Water: Spectral Deconvolution of Adsorbed Species. *J. Phys. Chem. Lett.* **2014**, *5*, 4194–4200.

(25) Moore, J. K.; Sakwa-Novak, M. A.; Chaikittisilp, W.; Mehta, A. K.; Conradi, M. S.; Jones, C. W.; Hayes, S. E. Characterization of a Mixture of CO_2 Adsorption Products in Hyperbranched Aminosilica Adsorbents by ^{13}C Solid-State NMR. *Environ. Sci. Technol.* **2015**, *49*, 13684–13691.

(26) Forse, A. C.; Milner, P. J.; Lee, J.-H.; Redfearn, H. N.; Oktawiec, J.; Siegelman, R. L.; Martell, J. D.; Dinakar, B.; Porter-Zasada, L. B.; Gonzalez, M. I.; et al. Elucidating CO_2 Chemisorption in Diamine-Appended Metal− Organic Frameworks. *J. Am. Chem. Soc* **2018**, *140*, 18016–18031.

(27) Mafra, L.; Cendak, T.; Schneider, S.; Wiper, P. V.; Pires, J.; Gomes, J. R. B.; Pinto, M. L. Structure of Chemisorbed CO_2 Species in Amine-Functionalized Mesoporous Silicas Studied by Solid-State NMR and Computer Modeling. *J. Am. Chem. Soc.* **2017**, *139*, 389–408.

Chapter 2: ^{13}C and ^{15}N NMR of $^{13}CO_2$ reacted APS-SBA15

This chapter is based on research described in two publications.

1. Title: Spectroscopic Characterization of Adsorbed $^{13}CO_2$ on 3-Aminopropylsilyl-Modified SBA15 Mesoporous Silica

Authors: Chia-Hsin Chen, Daphna Shimon, Jason J. Lee, Stephanie A. Didas, Anil K. Mehta, Carsten Sievers, Christopher W. Jones, Sophia E. Hayes

2. Title: ^{15}N Solid State NMR Spectroscopic Study of Surface Amine Groups for Carbon Capture: 3-Aminopropylsilyl Grafted to SBA-15 Mesoporous Silica

Authors: Daphna Shimon, Chia-Hsin Chen, Jason J. Lee, Stephanie A. Didas, Carsten Sievers, Christopher W. Jones, Sophia E. Hayes

In this chapter, solid-state NMR was used to interrogate the chemisorbed products of 3-aminopropylsilane functionalized mesoporous SBA15 silica [(APS)-SBA15], which captures CO_2 by chemisorption, using three hypothesized chemisorption reactions, shown in Scheme 2.1.[1] ^{15}N NMR is expected to be very informative in amine-SBA15 materials as it can confirm the reaction of amines and CO_2 forms carbamate. However, the natural abundance of ^{15}N is only 0.365 % which limits the routine use of ^{15}N NMR;so, isotopic enrichment is often a necessary step. ^{15}N enriched APS-SBA15 was synthesized and rotational-echo double-resonance (REDOR) experiments were used to probe the dipolar coupling between ^{13}C and ^{15}N enriched species.

(a)

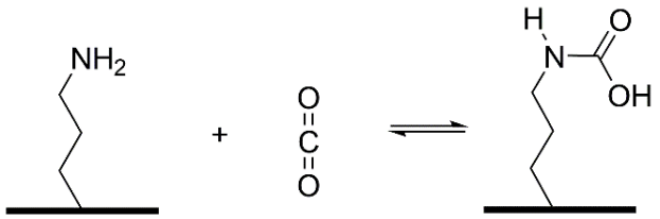

Carbamic acid

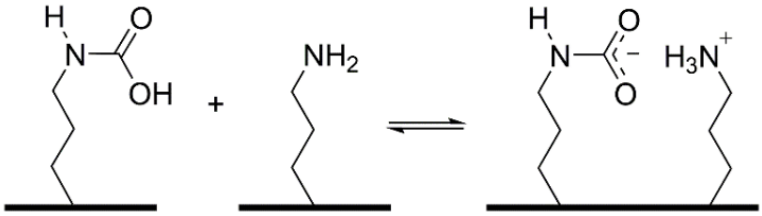

Ammonium carbamate ion pair

(b)

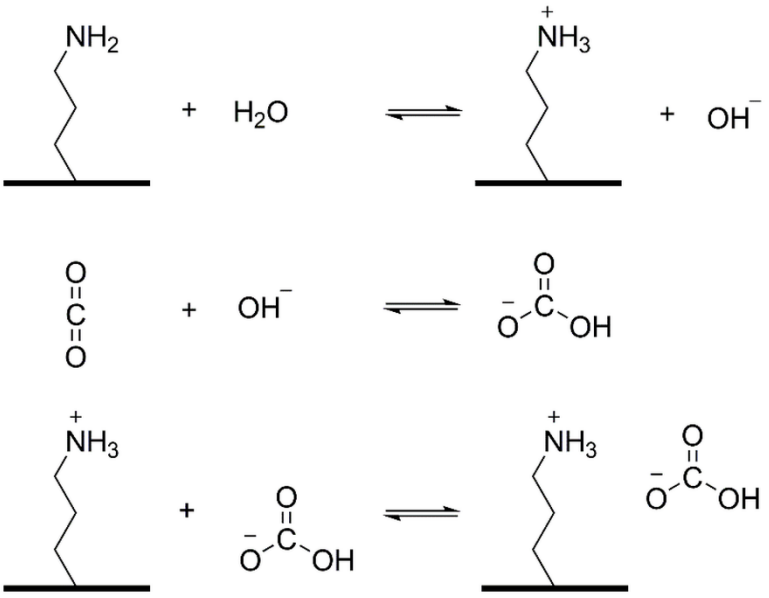

Ammonium bicarbonate

Scheme 2.1 (a) Hypothesized mechanism of carbamic acid and subsequent carbamate formation, and (b) Hypothesized mechanism of bicarbonate formation

2.1 Overview of $^{13}CO_2$ reacted APS-SBA15

Solid amine adsorbents are under development because of their low heat capacity and the relatively low threshold energy to desorb CO_2.[2] Amine modified mesoporous silica sorbents are promising materials being evaluated for the capture of CO_2 released from high-concentration point sources such as power plants. Research targeted at maximizing the efficiency of CO_2 uptake often focuses on the material itself, for example, tailoring different types of amines, varying the pore size of silica, and adjusting the amine density. Our goal is to study the interaction of CO_2 with the sorbent material at the molecular level, determining chemisorption products between CO_2 and amines to help maximize that efficiency.

The mechanism of aqueous amines reacting with CO_2 has been extensively studied.[2–5] When CO_2 becomes absorbed by primary and secondary amines in solution, a carbamate ion pair is formed.[2,4] In contrast, bicarbonate is the chemisorption product formed by tertiary amines, but only when water is present.[2,5] This second pathway to bicarbonates is also available to primary and secondary amines, yet it is much less favorable.[2] Compared to reactions in solution, reactions of CO_2 with solid amine adsorbents are more complicated as the solid-state host material's reactivity is influenced by several factors, including humidity, partial pressure of CO_2, and both the density and the nature of amine groups. These mesoporous systems are challenging to structurally characterize with conventional analytical techniques such as X-ray diffraction due to the lack of crystallinity. FTIR and solid-state NMR are two spectroscopic techniques that can provide information about structure, especially the local coordination environment of chemical moieties present in CO_2 chemisorption products, even in amorphous and surface-bound sites.

The identification of CO_2 chemisorption products is complicated by multiple reaction products that can form, including two types of carbamate[6] (an ion-paired species with an ammonium

propylsilane moiety, termed “ammonium carbamate ion pair,” and a surface-coordinated carbamate “silylpropylcarbamate”) as well as bicarbonate.[7] Bicarbonate was not found in several previous studies,[6,8–11] and this species has only been previously observed when the amine groups are present at low concentrations (termed “low loading”) in parallel with ammonium carbamate ion pairs.[7] In a recent study employing *in-situ* FTIR spectroscopy, multiple adsorbed CO_2 species were postulated.[12] The similarity of the vibrational stretching frequencies of the important C=O, NH_3^+, and COO^- groups in FTIR spectra creates a situation where the experimental spectra are complex and difficult to interpret.

Solid-state NMR is a complementary tool, particularly well-suited for amorphous or disordered materials that can provide quantitative information about the adsorption products since such species (C=O, NH_3^+, and COO^-) are distinct in NMR. For example, in a recent study of an amine-modified mesoporous silica sorbent (a hyperbranched aminosilica,)[13] two overlapping CO_2 chemisorption products were distinguished by the multiple transverse relaxation times (T_2) of a carbon peak where the 2 resonances were overlapped.[14]

2.2 Experimental section

[^{15}N] APS-SBA15 was synthesized by Jason Lee, a collaboration with Dr. Christopher Jones at Georgia Institute of Technology, using a literature procedure previously developed in their group.[15] $^{15}NH_3$ (g) was used to aminate a 3-bromopropylsilane grafted SBA15. The sample was sent to Atlantic Microlabs (Norcross, GA, USA) for elemental analysis to ensure that no bromine was left in the sample. The amine loading of [^{15}N] APS- SBA15 is 1.5 mmol N/g.

[^{15}N] APS-SBA15 was activated through drying at 110 °C under vacuum at 40 mTorr for 4 h in a round bottom flask using a Schlenk line, subsequently cooled to room temperature, and then transferred to a continuous-flow nitrogen-purged glove bag. Samples were packed into zirconia

NMR rotors under N_2 gas (to reduce water exposure from humidity). For $^{13}CO_2$ loading, the rotor was placed in a glass tube and connected to a gas manifold. The sample was then evacuated to 40 mTorr and dosed with 1 atm $^{13}CO_2$ for 10 h.

$^{15}N\{^1H\}$ CPMAS NMR experiments were performed on an Oxford 89 mm bore 6.93 T superconducting magnet with a Tecmag (Houston, TX) console equipped with a 4 mm HXY MAS Chemagnetics probe operating at ^{15}N and ^1H frequencies of 29.90 MHz and 294.97 MHz, respectively. The initial ^1H CP $\pi/2$ pulse length was 6 μs (evacuated sample) or 2 μs (CO_2 loaded sample), the ^1H-^{15}N cross-polarization Hartman-Hahn contact time was 0.5 ms with an RF field of ~17-20 kHz, and a recycle delay of 2 s. The magic-angle spinning rate was controlled at 5 kHz.

$^{13}C\{^1H\}$ CPMAS NMR and rotational-echo double-resonance (REDOR) were collected with a 14.1 T Bruker superconducting magnet and a Bruker AQS spectrometer equipped with a 4 mm HCN Biosolids probe with ^{13}C, ^{15}N and ^1H frequencies of 150.9 MHz, 60.81 MHz, and 600.13 MHz, respectively (collected at Emory University, in collaboration with Dr. Anil Mehta). The magic-angle spinning rate was controlled at 10 kHz. The probe exit temperature air was set to be below 0 °C to stabilize chemisorbed products during acquisition. The initial ^1H CP $\pi/2$ pulse width was 1.9 μs, ^1H-^{13}C cross-polarization Hartman-Hahn contact time was 3 ms with a ^1H RF field ramped over from the -1 to +1 sideband Hartman-Hahn CP match condition and a ^{13}C CP RF field of 62.5 kHz. The ^1H-^{15}N cross-polarization Hartman-Hahn contact time was 1 ms with an ^1H RF field ramped over from the -1 to +1 sideband Hartman-Hahn CP match condition and a ^{15}N CP RF field of 50 kHz. ^{13}C π-pulse widths were 4 μs and ^{15}N π-pulse widths were 8 μs. $^{15}N\{^{13}C\}$ and $^{13}C\{^{15}N\}$ REDOR π-pulses used xy-8 phase cycling[16], and EXORCYCLE phase cycling[17] of the final Hahn-echo refocusing pulse was used to minimize artifacts from RF-homogeneity.[18,19] SPINAL-64 ^1H decoupling[20] was used during both REDOR evolution and acquisition. The

observed-spin refocusing pulses were centered every rotor cycle, and the dephase-spin pulses were centered half-way through the rotor period, for maximum dephasing. $^{15}N/^{13}C$ pulse widths were optimized for each sample by choosing the pulse width that provided the maximum intensity where the pulse width was arrayed for a fixed RF field strength with a 54.4 ms REDOR full echo (S_0) experiment. ^{13}C chemical shifts were referenced using adamantane as an external reference with the –CH resonance set to 38.48 ppm[21] and ^{15}N chemical shifts were set using spectra were referenced (with respect to liquid NH_3 at 0 ppm) using the unified scale applying a $^{15}N/^{1}H$ ratio of 0.10132912.[22]

2.3 ^{15}N NMR of $^{13}CO_2$ reacted [^{15}N] APS-SBA15

The ^{15}N CPMAS NMR spectrum of ^{15}N isotopically enriched APS-SBA15 ([^{15}N] APS-SBA15) is complex, consisting of 3 resonances before exposure to $^{13}CO_2$(g) (Figure 2.1a) and 4 resonances after (Figure 2.1b) as summarized in Table 2.1. After $^{13}CO_2$ exposure, a new resonance becomes apparent at 88 ppm in the ^{15}N spectrum, and it is assigned on the basis of its chemical shift, to one

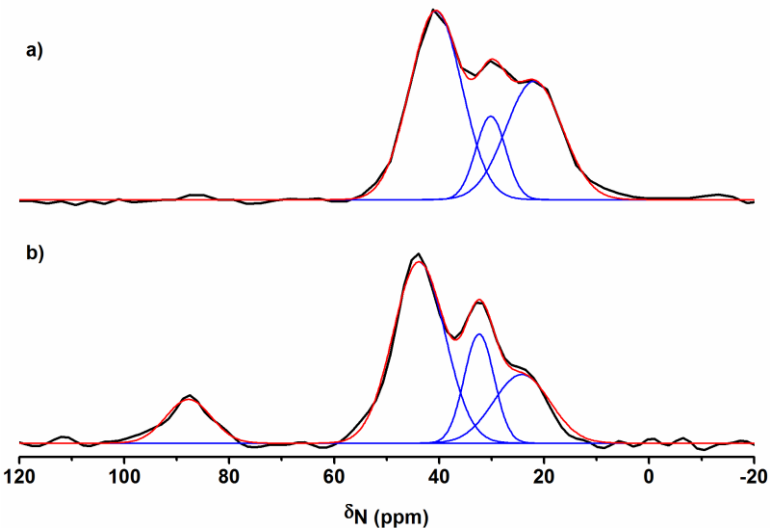

Figure 2.1 $^{15}N\{^{1}H\}$ CPMAS of [^{15}N] APS-SBA15 (a) before and (b) after $^{13}CO_2$ chemisorption adsorption referenced to NH_3 at 0 ppm. The spectra were deconvoluted into multiple Gaussian peaks listed in Table 2.1.

or more carbamate species.[23–26] The resonances at 24 ppm and 32 ppm are assigned to pendant aminopropylsilane (APS) groups, and have different relative intensities before and after loading $^{13}CO_2$. The 24 ppm resonance decreases in intensity, consistent with the reaction of $^{13}CO_2$ with the primary amine of [^{15}N] APS-SBA15, forming carbamate (see Scheme 2.1a), and is therefore assigned to the primary amine nitrogen of [^{15}N] APS-SBA15.[27] The resonance at 32 ppm increases slightly in intensity with CO_2 exposure, relative to other moieties, and is thus assigned to the ammonium propylsilane nitrogen [25,26,28] that is ion-paired to carbamate (or bicarbonate, as shown in Scheme 2.1b). An ammonium propylsilane species ion paired with adsorbed CO_2 would have

decreased mobility, leading to less averaging of the ^{15}N-^{1}H dipolar coupling, thereby enhancing such rigid groups in the experiment. It is worthwhile to note that the ammonium propylsilane present may also arise from protonation by the silanol groups and residual water on the silica surface.[29] The pendant APS species have been previously shown to hydrogen bond with such silanol groups.[30] Notably, the ^{15}N resonance at 44 ppm is not found in samples of APS-SBA15 synthesized by the more traditional route, via grafting 3-aminopropyl silane species,[12] yet its chemical shift is consistent with an alkyl amine.[31] Post-grafting amination was conducted by grafting bromopropylsilanes onto the surface of SBA15 and reacting it with ammonia gas. It is possible that a newly-formed alkyl amine (APS) can attack a neighboring bromopropylsilane and form a di-tethered species, which is a secondary amine (Scheme 2.2). Furthermore, primary amines are also nucleophiles and can compete with the ammonia gas to react with the bromopropylsilanes.[32] Therefore, this resonance at 44 ppm is likely a byproduct of the [^{15}N] APS-SBA15 synthesis used here, whereby alkyl halide groups are reacted with ammonia by post-grafting amination to create alkylamine groups.[15] More evidence to support the presence of

Table 2.1. ^{15}N CPMAS chemical shift of $^{13}CO_2$ reacted [^{15}N] APS-SBA15 and the cross-polarization buildup time constant, T_{IS}.

Chemical species	^{15}N isotropic chemical shift (ppm)	T_{IS} (msec)
Aminopropylsilane	24	0.21±0.02
Ammonium propylsilane	32	0.27±0.06
Ditethered amine	44	0.13±0.01
Carbamate	88	0.09±0.02

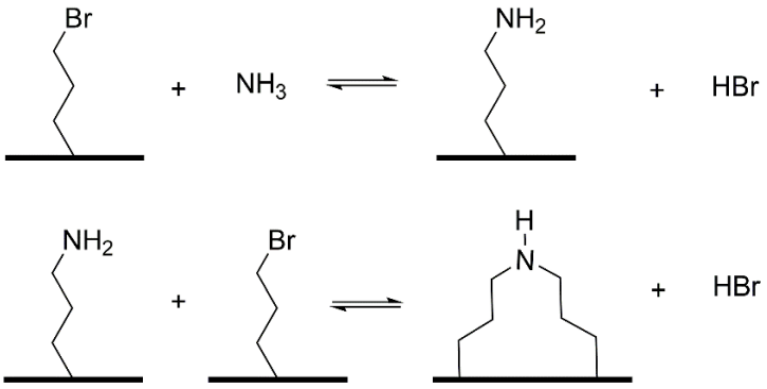

Scheme 2.2 Hypothesized mechanism of formation of ditethered amines.

detethered amines is the elemental analysis of [^{15}N] APS-SBA15 shown in Table 2.2. The expected carbon-to-nitrogen ratio of APS is 3-to-1, however, the [^{15}N] APS-SBA15 shows a ratio of 5.5-to -1 indicating more carbon than expected in the sample. The carbon to nitrogen ratio of a ditethered amine is expected to be 6-to-1. The unexpected carbon to nitrogen ration suggests that there are mixtures of APS and ditethered amines in the [^{15}N] APS-SBA15.

	C (mmol/g)	N (mmol/g)	C/N
[^{15}N] APS-SBA15	8.5	1.5	5.5

Table 2.2 Elemental analysis of [^{15}N] APS-SBA15 (performed by Atlantic Microlabs (Norcross, GA, USA))

The cross polarization build-up time constants (T_{IS}) are determined through fitting of the ^{15}N{^{1}H} contact time curve in the CPMAS experiment with the equation by Mehring, and are reported in Table 2.1.[33] Shorter T_{IS} values indicate a stronger dipolar interaction between nitrogen and protons; the strength of the interaction is distance dependent and can also vary with dynamic motion, such that a more rigid (less dynamically averaged) structure will lead to a stronger dipolar interaction. The T_{IS} of the nitrogen-bearing byproduct (at 44 ppm) is shorter than that of the aminopropylsilane

and the ammonium propylsilane groups, which indicates a stronger dipolar interaction between the nitrogen and proton(s) and supports the idea of a more rigid structure than aminopropylsilane. The T_{IS} time constant of the carbamate is also shorter than that of the aminopropylsilane and the ammonium propylsilane groups, even though the N-H bond distance(s) should be relatively similar, suggesting that when the carbamate is ion paired (or hydrogen-bound to the surface), it is less mobile.

2.4 $^{15}N\{^{13}C\}$ REDOR and $^{13}C\{^{15}N\}$ REDOR of $^{13}CO_2$ reacted [^{15}N] APS-SBA15

The ^{15}N-^{13}C bond in carbamate -- assigned to the ^{15}N resonance at 88 ppm in the $^{13}CO_2$-adsorbed [^{15}N] APS-SBA -- was evaluated by measuring the dipolar coupling with a $^{15}N\{^{13}C\}$ REDOR experiment[34,35] with ^{1}H decoupling. The REDOR experiment reintroduces the ^{15}N-^{13}C dipolar coupling that is averaged to zero by magic-angle spinning (MAS) used in $^{15}N\{^{1}H\}$ CPMAS (Figure 2.1). REDOR data are collected in two sets of experiments, one with rotor-synchronized spin-echo π-pulses on the so-called "observed" spin (^{15}N) resulting with the full-echo (S_0) spectra and a second set of experiments with dephasing π-pulses on the ^{13}C spins (termed "S"). The rotor-synchronized ^{13}C π-pulses in the S spectra reintroduce the dipolar interactions between ^{15}N and ^{13}C spins. The intensity differences between the S_0 (full-echo) and S (dephased) spectra (ΔS) are directly related to the ^{15}N-^{13}C dipolar coupling. When plotted (see Figure 2.2) as $\Delta S/S_0$ to account for ^{15}N (observe-spin) relaxation as a function of REDOR evolution time, the $^{15}N\{^{13}C\}$ REDOR data (Figure 2.2) fit well to an isolated ^{15}N-^{13}C spin-pair separated at a distance of 1.45 Å, consistent with a ^{15}N-^{13}C bond found in amide-like species such as carbamate and carbamic acid.[23,24,36] It is worthwhile to note here that the REDOR data, approaching a value of $\Delta S/S_0$ of $\approx$1.0, suggests that there is little or no exchange of ^{12}C for ^{13}C on the timescale of these NMR experiments (5 to 7 days).

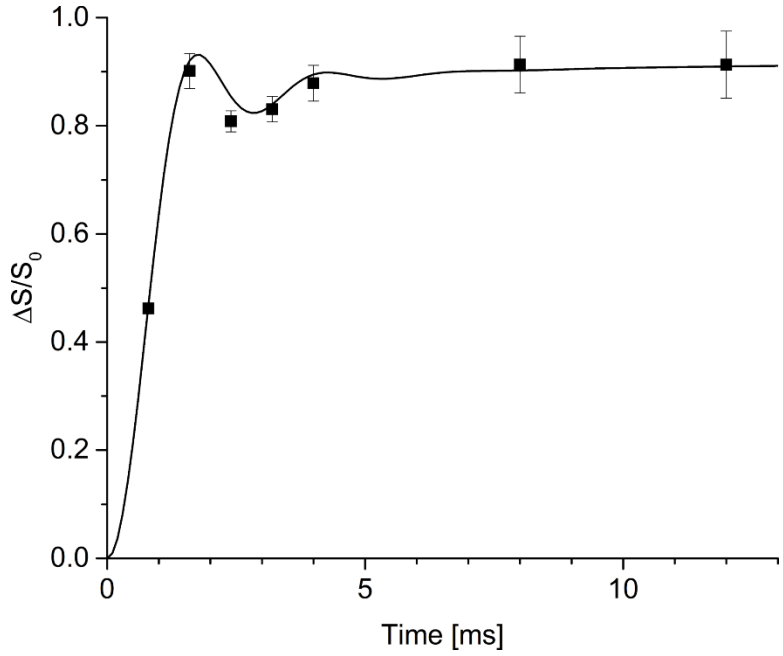

Figure 2.2 $^{15}N\{^{13}C\}$ REDOR dephasing of [^{15}N] APS-SBA15 reacted with $^{13}CO_2$ for the ^{15}N 88 ppm resonance (shown in Figure 2.1b.) The solid line is the fit to the data corresponding to a $^{15}N–^{13}C$ distance of 1.45 Å, as described in the text.

The ^{13}C spectrum of the $^{13}CO_2$-adsorbed [^{15}N] APS-SBA15 is dominated by the chemisorption product of $^{13}CO_2$; shown in Figure 2.3. Even though a single resonance is seen for ^{15}N chemisorption product(s), two strongly-overlapped ^{13}C carbon resonances are found. The 164 ppm ^{13}C resonance can be deconvoluted into two resonances centered at 161 ppm and 165 ppm, indicating the presence of at least two chemisorbed reaction products. The less intense resonance at 161 ppm has been assigned based on previous studies to carbamic acid (RNCOOH.)[37] The chemical shift of the more intense resonance at 165 ppm is consistent with carbamate ($RNCOO^-$,)[2] yet is challenging to definitively assign because of the similarity of the chemical shifts of carbamate and bicarbonate carbons at 164.2 ppm[24] and 163.8 ppm,[38] respectively. Both carbamate and bicarbonate can be formed under the experimental conditions employed here, where the

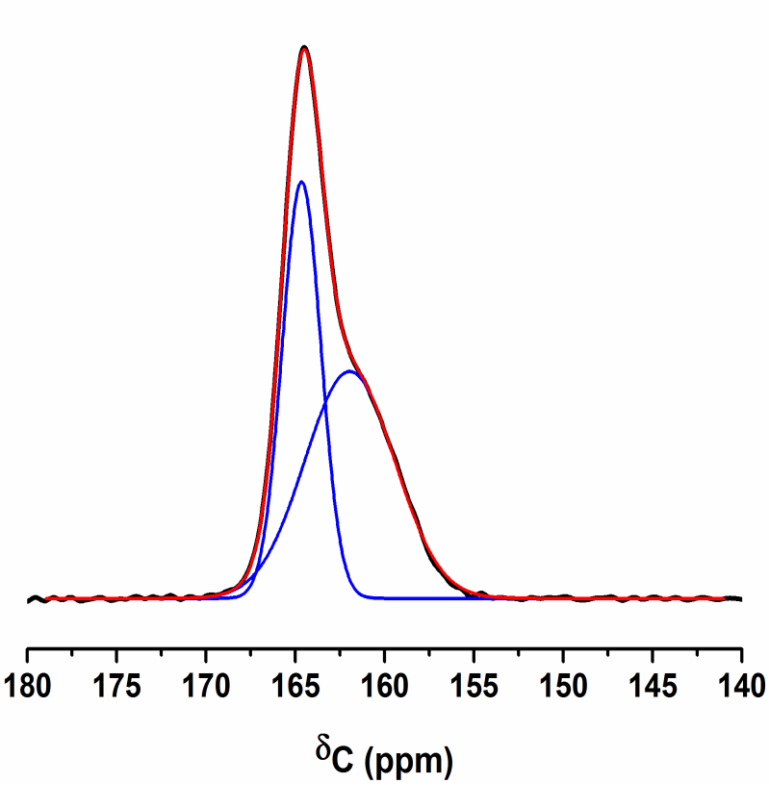

Figure 2.3 Expanded region of $^{13}C\{^{1}H\}$ CPMAS NMR spectra of $^{13}CO_2$ adsorbed [^{15}N] APS-SBA15. Blue lines are deconvolution of spectral line shape to two resonances, red is the sum of these two Gaussians, and black is experimental data.

samples contain surface water, and humidity was not rigorously excluded. Assignments based on isotropic chemical shift alone are tenuous, as the solution-phase isotropic chemical shift of bicarbonate is highly pH dependent.[39] Owing to their similar chemical motifs, carbamate chemical shifts may also be similarly pH dependent. Therefore, the resonance at 165 ppm is potentially carbamate, bicarbonate, or both species given their nearly indistinguishable isotropic chemical shifts (< 1 ppm difference). These assignments were therefore evaluated using coupling from ^{13}C to neighboring ^{15}N spins through REDOR.

$^{13}C\{^{15}N\}$ REDOR dephasing (where ^{13}C is the observed spin) of the 165 ppm resonance (Figure 2.4) fits well to a ^{13}C spin next to two ^{15}N spins (a three-spin model[40,41]), with one ^{13}C-^{15}N distance of 1.42 Å, and the second ^{13}C-^{15}N distance of 3.13 Å. The ^{13}C-^{15}N distance of 1.42 Å is consistent

with the direct single C-N bond of carbamate that was observed in $^{15}N\{^{13}C\}$ REDOR (Figure 2.2). The more distant ^{15}N site is most likely from an ammonium propylsilane ion coordinated with carbamate. The possibility of the second ^{15}N being a neighboring carbamate can be excluded because $^{15}N\{^{13}C\}$ REDOR (Figure 2.2) fits well to a single ^{15}N-^{13}C dipolar-coupled spin-pair, indicating each carbamate is isolated from other similar species.

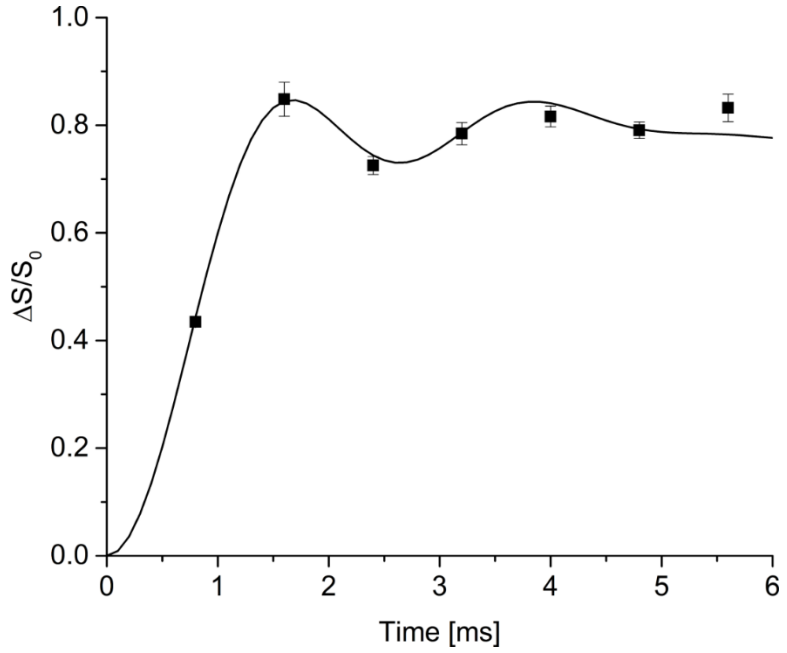

Figure 2.4 $^{13}C\{^{15}N\}$ REDOR of [^{15}N] APS-SBA reacted with $^{13}CO_2$. The REDOR dephasing of $\Delta S/S_0$ versus the dipolar evolution time is shown for the ^{13}C 165 ppm resonance that arises after reaction with $^{13}CO_2$. Fits to the data are shown as solid lines and described in the text.

In the $^{13}C\{^{15}N\}$ REDOR fits, only 90% of the maximum dephasing is reached for the carbamate 165 ppm species. As nearly all ^{13}C-^{15}N pairs that are formed are isotopically enriched by the introduction of $^{13}CO_2$ gas to make the enriched chemisorbed product, and ^{15}N of [^{15}N] APS-SBA15 is enriched at ~98%, the "missing" 10% of the expected intensity at 165 ppm must come from ^{13}C spins that are not proximal to ^{15}N spins. We suggest three plausible hypotheses to account for the uncoupled ^{13}C spins:

1) During synthesis of [^{15}N] APS-SBA15, 10% of the ^{15}N has exchanged with natural abundance nitrogen (^{14}N) leading to carbamates that are not isotopically enriched; the ^{13}C-^{14}N carbamate dipolar coupling is not recoupled in the ^{13}C{^{15}N} REDOR experiment.
2) The C-N bond is present on a moiety that is undergoing motion that averages the ^{13}C-^{15}N dipolar coupling to zero, making it invisible in the ^{13}C{^{15}N} REDOR experiment.
3) Another ^{13}C species is present with a chemical shift at 165 ppm that does not have a ^{13}C-^{15}N bond, such as a bicarbonate, $H^{13}CO_3^-$.

The first hypothesis, that ^{14}N can exchange for ^{15}N, is addressed first, considering the chemical route for ^{14}N incorporation. One possible source of ^{14}N in the synthesis of [^{15}N] APS-SBA15 comes from the filtration step. The sample was filtered after the amination and washed with an ammonium hydroxide solution to remove HBr formed as a side product. If some unreacted bromopropylsilane pendant molecules were present on SBA-15, one might hypothesize that they could react with ^{14}N ammonium hydroxide, to form ^{14}N aminopropylsilane. However, NH_4^+ is a poor nucleophile, and such a reaction at low temperature and with brief exposure is highly unlikely.

We address the second hypothesis, that the loss of ^{13}C{^{15}N} REDOR intensity at the dephasing maximum is due to motional averaging of the ^{13}C-^{15}N dipolar coupling to zero. We note that no loss is observed in the complementary ^{15}N{^{13}C} REDOR dephasing maximum (Figure 2.2). This finding shows that all ^{15}N present as carbamate is directly bonded to ^{13}C, indicating that the ^{13}C-^{15}N bond has little motion that leads to an average dipolar coupling of zero, and allows us to discount this hypothesis.

Taken together, this evidence suggests the third hypothesis is the most likely, and we posit that 10% of the signal at 165 ppm is carbon that is not bound to nitrogen, with bicarbonate being the

most likely candidate. A possible criticism of this assignment can be anticipated, namely that bicarbonate (an anion) should have weak coupling to a neighboring cation, such as ammonium propylsilane.

Nevertheless, the potentially distant coupling of ^{13}C bicarbonate to a neighboring ^{15}N would be weak given the long through-space C-N distance, and in very low concentration. Prior work of detection of bicarbonate species by FTIR spectroscopy suggested such species form in relatively small amounts compared to carbamate species.[7] In addition, bicarbonate may be paired with an entirely different cationic species in APS-SBA, such as H_3O^+.[42,43] Prior studies have shown spectra of humid CO_2 on bare silica, where it appears that there is a carbonate-like species forming with just CO_2/water on SBA15.[7] However, due to the large surface coverage of amines on the silica sorbent, there should be little to no free hydroxyl groups with which CO_2 can interact, making it unlikely that carbonate-like species form on the [^{15}N] APS-SBA15 material.

A recent study[44] on a related material paints a different picture of a chemisorbed CO_2 species. Instead of carbamate, this other study assigns all species to various carbamic acid moieties. We note that this system utilizes a different host material and a slightly different grafting agent (SBA-15 functionalized with 3-aminopropyltriethoxysilane, "APTES"). An important contrast to this other study is that our ^{15}N data and our IR spectra indicate the presence of both amine and ammonium propylsilane groups, whereas this APTES study found only amines present, demonstrating a key difference between our two systems.

2.5 Desorption of CO_2

While CO_2 adsorption has been shown to result in carbamate, carbamic acid, and possibly other chemisorption products, this reaction is thermodynamically reversible.[11,45–48] CO_2 can be released over time, typically under conditions of heat and vacuum that favor desorption and often lead to

urea formation.[47,48] While CPMAS is inherently not quantitative, at a constant (cross-polarization) contact time, the relative intensities of the resonances can be helpful for monitoring

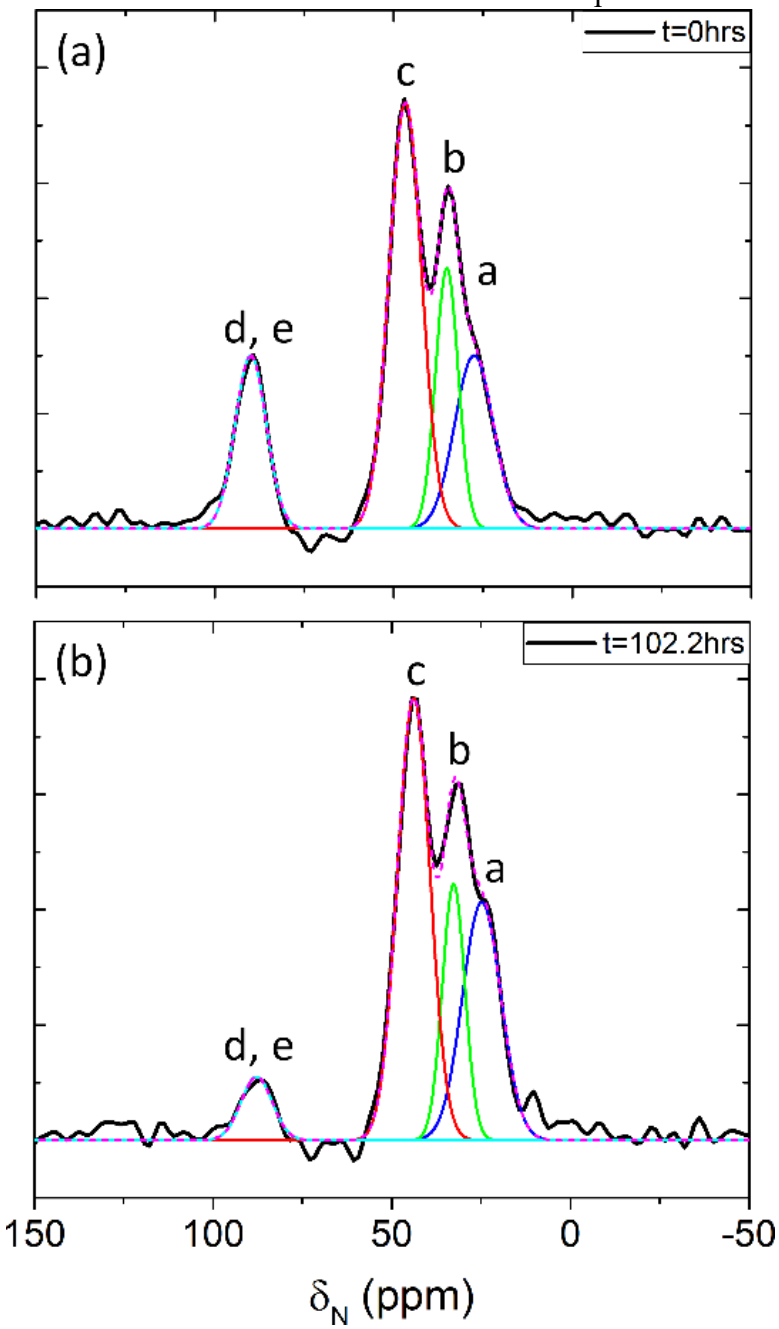

Figure 2.5 $^{15}N\{^{1}H\}$ CPMAS NMR spectra of [^{15}N]APS-SBA15, measured at two times, t, after loading CO_2 gas into the sample. The spectra were recorded at (a) t=0 hrs (b) and t=102.2 hrs. The experimental spectra are shown in black, overlaid with the sum of a;; the fitted Gaussian peaks in dashed-line magenta. The peaks are assigned: 3-aminopropylsilane (blue), ammonium propylsilane (green), ditethered secondary amine (red), and chemisorbed products (cyan).

the sample evolution as a function of time. Thus, we are able to monitor the changes occurring during CO_2 desorption using $^{15}N\{^1H\}$ CPMAS. In this work, the desorption happened spontaneously. In Figure 2.5, we plot two spectra of the $^{13}CO_2$-exposed [^{15}N] APS-SBA15 at two different times after $^{13}CO_2$ exposure: 0 h and 102.2 h. In this case an o-ring spacer was placed inside the NMR rotor to slow down the release of CO_2 from the sample space during the experiment (maintaining an atmosphere of released CO_2 gas). Comparing spectra recorded immediately after CO_2 loading, and 102.2 h later, there are changes in the intensities of the different ^{15}N resonances, without normalizing the spectra. In particular, the product resonance (d, e ≈ 88ppm) decreases, while the aminopropylsilane resonance (a, 24 ppm) increases.

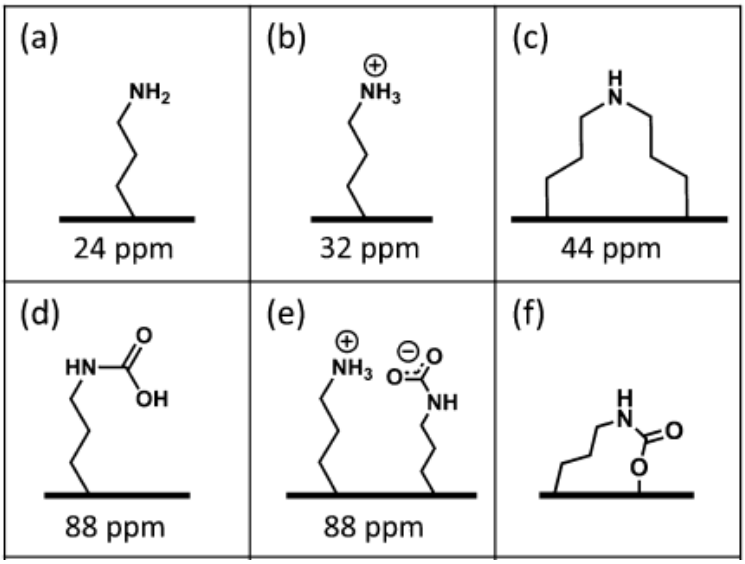

Scheme 2. Chemical structures of species in the [^{15}N] APS-SBA15 and their ^{15}N chemical shift. (a)3-aminopropylsilane, (b) ammonium propylsilane, (c)ditethered secondary amine, (d)carbamic acid ,(e) ammonium carbamate and (f) surface carbamate

Using the integrated intensities extracted from the deconvoluted $^{15}N\{^1H\}$ CPMAS spectra, the change in the resonance intensities as a function of time can be monitored, as plotted in Figure 2.6. Figure 2.6 depicts the total ^{15}N intensity (the sum of the integrated intensity from all resonances), which has a very slight negative slope-- an unsurprising observation for such long NMR

experiments (where loss of RF tuning and diminution of the optimal CP conditions both contribute to this effect). Nevertheless, we do not expect a change in the total amount of ^{15}N in the sample during our experiments. To correct for this slight slope, the total decreasing intensity was fitted with a linear function. We then divided all the curves in Figure 2.6 by the linear function, thus deconvoluting the effect of the change in total intensity from the loss of CO_2 products as a function of time. The corrected curves are plotted in Fig. 2.6b, where the amplitudes of the curves are plotted as a fraction of change of each curve.

Examining Fig. 2.6b, it is clear that the chemisorbed product intensity and the 3-aminopropylsilane intensity change concurrently, and with a similar timescale. We note that the fractional change between the product resonance (decrease) and the 3-aminopropylsilane resonance (increase) differ slightly. However, given the low signal-to-noise ratio of the latter, it is difficult to assess with certainty if this effect is real.

Also in Fig. 2.6b, we see that the ditethered secondary amine intensity, as well as the sum of the 3-aminopropylsilane, ammonium propylsilane and chemisorbed product intensities can be considered constant during this experiment. It may be surprising that the ditethered secondary amine does not react with CO_2, as there are reports in the literature that show carbamate formation on secondary amines. The difference here may be the rigidity of the ditethered secondary amine (as shown by the ^{15}N contact time curve), making it less likely to react with CO_2 than the singly-tethered secondary amines discussed in the literature, perhaps due to difficulty in interacting with a second N-bearing group to accept a proton from a carbamic acid intermediate.

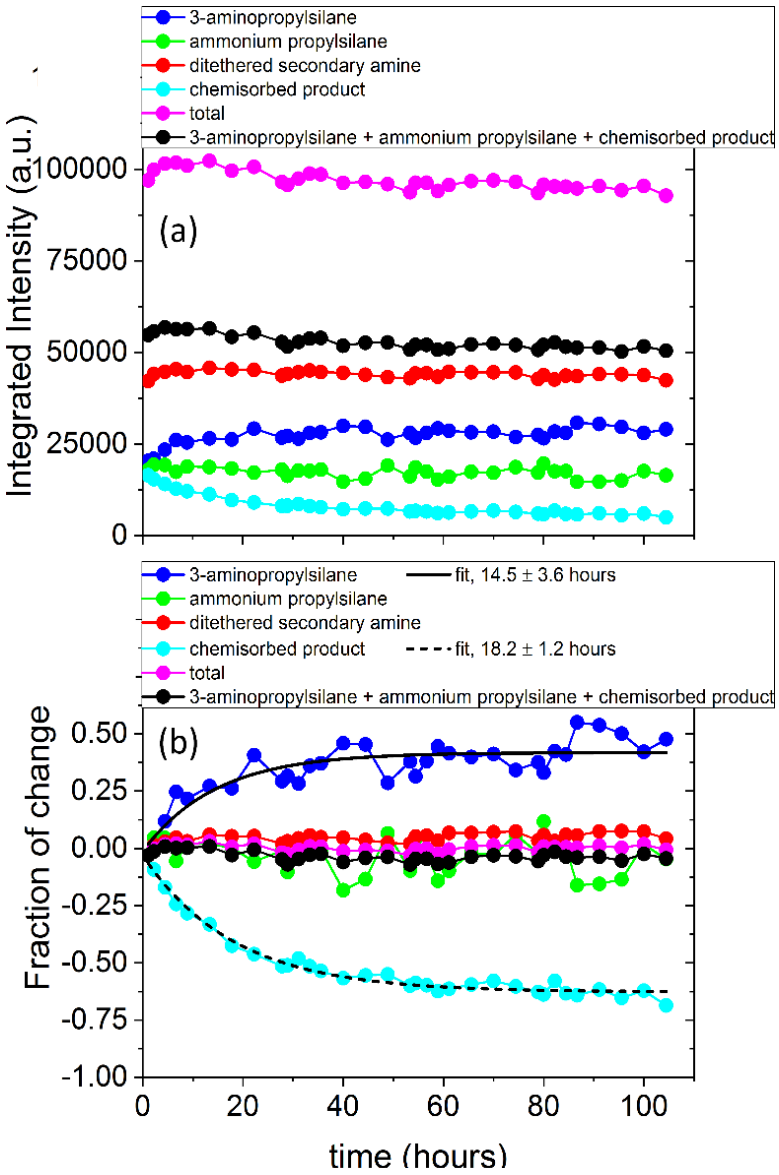

Figure 2.6 Integrated intensities of different ^{15}N peaks as a function of time, t, after loading CO_2 gas into the [^{15}N] APS-SBA15 sample. The peaks are assigned to: 3-aminopropylsilane (blue, a), ammonium propylsilane (green, b), ditethered secondary amine (red, c), chemisorbed product (cyan, d and e), total intensity (magenta), and the sum of 3-aminopropylsilane + ammonium propylsilane + chemisorbed products (black). (a) Integrated intensity in a.u. and (b) fraction of change of the intensity overlaid with the fitting to single exponential functions (black lines).

It is curious to note that the ammonium propylsilane signal does not change as a function of time. This is unexpected for several reasons. This protonated form of APS is believed to ion-pair with carbamate;[12] yet counterintuitively, when the chemisorbed product is lost over time, this resonance remains constant. In a recently published paper, we showed the ^{15}N spectrum of ~1.5 mmol N/g ^{15}N-APS SBA15 sample before and after loading with CO_2 (the "before" spectrum was heated under vacuum as described in the Materials and Methods section).[49] The data show that when CO_2 is loaded into the sample, we saw a decrease in the 3-aminopropylsilane resonance, and an increase in the ammonium propylsilane and the chemisorbed product resonances. This suggests that the formation of the carbamate is stabilized by ammonium proplysilane when CO_2 is introduced into the sample (note that the $^{13}C\{^1H\}$-CPMAS of the same sample showed the formation of both carbamate and carbamic acid).[49] This leads to the question: upon the loss of chemisorbed product, why is the ammonium propylsilane not changing? As such, there are several possible explanations for what is taking place in our sample:

1. The fact that the ammonium propylsilane signal persists when CO_2 is removed from the sample suggests that ammonium carbamate is not lost during CO_2 desorption. Therefore, it is likely that at least two nitrogen-bearing products are formed when CO_2 is introduced into the sample, and we cannot resolve the two using ^{15}N-NMR at 7T (both appear at 88 ppm). One of the products has previously been assigned as carbamate (see Scheme 2.2, species e). The second product is likely carbamic acid (see Scheme 2.2, species d) (also seen in the ^{13}C spectrum), but could also be surface bound carbamate (see Scheme 2.2, species f).[49]
    a. Carbamic acid: As can be seen in Scheme 2.1, carbamic acid is not ion-paired to any ammonium propylsilane groups; therefore, its desorption would not result in

a change in the ammonium propylsilane. Carbamic acid is known to be less stable than ammonium carbamate[9,14,23,37] and, therefore, it would make sense that carbamic acid would be the dominant species lost in Figure 2.6, leaving behind ammonium carbamate.

b. Surface bound carbamate: The second species is a surface-bound carbamate that is not stabilized by proplyammonium. In this case, the proplyammonium would be independent from the surface bound carbamate, and therefore, its concentration would remain flat. However, there is no reason to expect that surface-bound carbamate would be less stable that ammonium carbamate during desorption. Moreover, surface-bound carbamate has been shown to form at low APS concentrations, but not at higher concentrations due to steric hindrance.[6,8]

2. Another less likely scenario is that the carbmate that has been formed is able to convert to bicarbonate. In the presence of water, bicarbonate is known to form, and could act to stabilize the ammonium propylsilane. We have shown that bicarbonate is formed in small quantities during $^{13}CO_2$ chemisorption.[49] The bicarbonate would not be visible in a $^{15}N\{^{1}H\}$-CPMAS experiment because it does not contain a nitrogen, but this conversion from carbamate to bicarbonate would result in no change in the proplyammonium intensity (and a decrease in the chemisorbed product resonance at ^{15}N 88 ppm).

In ^{13}C solid-state NMR, two resolved peaks are observed in the region that corresponds to carbamate and carbamic acid;[49] however, only one ^{15}N resonance is discernable here. With this additional knowledge provided by ^{13}C, and given the discussion above, vide infra, the product ^{15}N resonance (88 ppm) is attributed to two species, ammonium carbamate and carbamic acid.

2.6 Conclusion

In summary, we have found the chemisorption products of $^{13}CO_2$ reacting with [^{15}N] APS-SBA15 are comprised of carbamic acid, carbamate, and a carbon moiety that lacks any adjoining nitrogen, which we assign to bicarbonate. The combination of $^{15}N\{^{13}C\}$ REDOR and its counterpart, $^{13}C\{^{15}N\}$ REDOR, makes a compelling case for such an assignment. $^{15}N\{^{13}C\}$ REDOR shows that the carbamate nitrogen species are subject to a *single* ^{15}N-^{13}C distance consistent with a directly bonded pair. In contrast, $^{13}C\{^{15}N\}$ REDOR (at the resonance frequency where both carbamate and bicarbonate overlap) shows carbon interacting with multiple ^{15}N sites—a directly-bonded ^{13}C-^{15}N pair, and a more distant interaction, likely an ammonium propylsilane moiety with which the carbamate would ion pair. The $^{13}C\{^{15}N\}$ REDOR dephasing did not build up to the full 100% intensity that is expected, and the significance is that the "missing" intensity would be attributable to ^{13}C resonating at 165 ppm and not in dipolar contact with ^{15}N. Bicarbonate is a species that is consistent with these findings and has been previously identified by FT-IR in related work,[7] and proior studies of (related) hyper-branched amino silica solid amine sorbet.[14]

The synthetic route for preparation of the ^{15}N-enriched APS is different from other preparations, and NMR spectroscopy was used previously[12] to examine structural differences between the natural abundance and enriched samples. A new ^{15}N resonance that was observed in the amine region has been assigned to a di-tethered amine.

References (Chapter 2)

(1) *The Byproduct Urea Is Not Considered in This Study Because the Reaction Was Conducted at Lower Temperature Conditions That Do Not Promote Its Formation.*

(2) Bollini, P.; Didas, S. A.; Jones, C. W. Amine-Oxide Hybrid Materials for Acid Gas Separations. *J. Mater. Chem.* **2011**, *21*, 15100–15120.

(3) Kortunov, P. V.; Siskin, M.; Baugh, L. S.; Calabro, D. C. In Situ Nuclear Magnetic Resonance Mechanistic Studies of Carbon Dioxide Reactions with Liquid Amines in Non-Aqueous Systems: Evidence for the Formation of Carbamic Acids and Zwitterionic Species. *Energy Fuels* **2015**, *29*, 5940–5966.

(4) Caplow, M. Kinetics of Carbamate Formation and Breakdown. *J. Am. Chem. Soc.* **1968**, *90*, 6795–6803.

(5) Donaldson, T. L.; Nguyen, Y. N. Carbon Dioxide Reaction Kinetics and Transport in Aqueous Amine Membranes. *Ind. Eng. Chem. Fundam.* **1980**, *19*, 260–266.

(6) Bacsik, Z.; Ahlsten, N.; Ziadi, A.; Zhao, G. Y.; Garcia-Bennett, A. E.; Martín-Matute, B.; Hedin, N. Mechanisms and Kinetics for Sorption of CO_2 on Bicontinuous Mesoporous Silica Modified with n-Propylamine. *Langmuir* **2011**, *27*, 11118–11128.

(7) Didas, S. A.; Sakwa-novak, M. A.; Foo, G. S.; Sievers, C.; Jones, C. W. Effect of Amine Surface Coverage on the Co-Adsorption of CO_2 and Water: Spectral Deconvolution of Adsorbed Species. *J. Phys. Chem. Lett.* **2014**, *5*, 4194–4200.

(8) Danon, A.; Stair, P. C.; Weitz, E. FTIR Study of CO_2 Adsorption on Amine Grafted SBA-15 : Elucidation of Adsorbed Species. *J. Phys. Chem. C* **2011**, *115*, 11540–11549.

(9) Yu, J.; Chuang, S. S. C. The Structure of Adsorbed Species on Immobilized Amines in CO_2 Capture: An in Situ IR Study. *Energy Fuels* **2016**, *30*, 7579–7587.

(10) Aziz, B.; Hedin, N.; Bacsik, Z. Quantification of Chemisorption and Physisorption of Carbon Dioxide on Porous Silica Modified by Propylamines: Effect of Amine Density. *Microporous Mesoporous Mater.* **2012**, *159*, 42–49.

(11) Wang, X.; Schwartz, V.; Clark, J. C.; Ma, X.; Overbury, S. H.; Xu, X.; Song, C. Infrared Study of CO_2 Sorption over "Molecular Basket" Sorbent Consisting of Polyethylenimine-Modified Mesoporous Molecular Sieve. *J. Phys. Chem. C* **2009**, *113*, 7260–7268.

(12) Foo, G. S.; Lee, J. J.; Chen, C.-H.; Hayes, S. E.; Sievers, C.; Jones, C. W. Elucidation of Surface Species through in Situ FTIR Spectroscopy of Carbon Dioxide Adsorption on Amine-Grafted SBA-15. *ChemSusChem* **2016**, *9*, 1–12.

(13) Hicks, J. C.; Drese, J. H.; Fauth, D. J.; Gray, M. L.; Qi, G.; Jones, C. W. Designing Adsorbents for CO_2 Capture from Flue Gas-Hyperbranched Aminosilicas Capable of Capturing CO_2 Reversibly. *J. Am. Chem. Soc.* **2008**, *130*, 2902–2903.

(14) Moore, J. K.; Sakwa-Novak, M. A.; Chaikittisilp, W.; Mehta, A. K.; Conradi, M. S.; Jones, C. W.; Hayes, S. E. Characterization of a Mixture of CO_2 Adsorption Products in Hyperbranched Aminosilica Adsorbents by ^{13}C Solid-State NMR. *Environ. Sci. Technol.* **2015**, *49*, 13684–13691.

(15) Moschetta, E. G.; Sakwa-Novak, M. A.; Greenfield, J. L.; Jones, C. W. Post-Grafting Amination of Alkyl Halide-Functionalized Silica for Applications in Catalysis, Adsorption, and ^{15}N NMR Spectroscopy. *Langmuir* **2015**, *31*, 2218–2227.

(16) Gullion, T.; Baker, D. B.; Conradi, M. S. New, Compensated Carr-Purcell Sequences. *J. Magn. Reson.* **1990**, *89*, 479–484.

(17) Rance, M.; Byrd, R. A. Obtaining High Fidelity Spin 1/2 Powder Spectra in Anisotropic Media: Phase Cycled Hahn-Echo Spectroscopy. *J. Magn. Reson.* **1983**, *54*, 221–240.

(18) Weldeghiorghis, T. K.; Schaefer, J. Compensating for Pulse Imperfections in REDOR. *J. Magn. Reson.* **2003**, *165*, 230–236.

(19) Sinha, N.; Schmidt-Rohr, K.; Hong, M. Compensation for Pulse Imperfections in Rotational-Echo Double-Resonance NMR by Composite Pulses and EXORCYCLE. *J. Magn. Reson.* **2004**, *168*, 358–365.

(20) Fung, B. M.; Khitrin, A. K.; Ermolaev, K. An Improved Broadband Decoupling Sequence for Liquid Crystals and Solids. *J. Magn. Reson.* **2000**, *142*, 97–101.

(21) Morcombe, C. R.; Zilm, K. W. Chemical Shift Referencing in MAS Solid State NMR. *J. Magn. Reson.* **2003**, *162*, 479–486.

(22) Harris, R. K.; Becker, E. D.; Cabral DE Menezes, S. M.; Granger, P.; Hoffman, R. E.; Zilm, K. W. Further Conventions for NMR Shielding. *Pure Appl. Chem.* **2008**, *80*, 59–84.

(23) Andreoli, E.; Dillon, E. P.; Cullum, L.; Alemany, L. B.; Barron, A. R. Cross-Linking Amine-Rich Compounds into High Performing Selective CO_2 Absorbents. *Sci. Rep.* **2014**, *4*, 7304.

(24) Hung, C.-T.; Yang, C.-F.; Lin, J.-S.; Huang, S.-J.; Chang, Y.-C.; Liu, S.-B. Capture of Carbon Dioxide by Polyamine-Immobilized Mesostructured Silica: A Solid-State NMR

Study. *Micropouous mesoporous Mater.* **2017**, *238*, 2–13.

(25) Maeda, S.; Oumae, S.; Kaneko, S.; Kunimoto, K. K. Formation of Carbamates and Cross-Linking of Microbial Poly(e-l- Lysine) Studied by ^{13}C and ^{15}N Solid-State NMR. *Polym. Bull.* **2012**, *68*, 745–754.

(26) Dos, A.; Schimming, V.; Tosoni, S.; Limbach, H.; Dos, A.; Schimming, V.; Tosoni, S.; Limbach, H. Acid - Base Interactions and Secondary Structures of Poly-L-Lysine Probed by ^{15}N and ^{13}C Solid State NMR and Ab Initio Model Calculations. *J. Phys. Chem. B* **2008**, *112*, 15604–15615.

(27) Perinu, C.; Saramakoon, G.; Arstad, B.; Jens, K.-J. Application of ^{15}N-NMR Spectroscopy to Analysis of Amine Based CO_2 Capture Solvents. *Energy Procedia* **2014**, *63*, 1144–1150.

(28) Ratcliffe, C. I.; Ripmeester, J. A.; Tse, J. S. ^{15}N NMR Chemical Shifts in Solid NH_4^+ Salts. *Chem. Phys. Lett.* **1983**, *99*, 177.

(29) Hahn, M. W.; Jelic, J.; Berger, E.; Reuter, K.; Jentys, A.; Lercher, J. A. Role of Amine Functionality for CO_2 Chemisorption on Silica. *J. Phys. Chem. B* **2016**, *120*, 1988–1995.

(30) Ghindes-Azaria, L.; Levy, E.; Keinan-Adamsky, K.; Goobes, G. Conformation and Dynamics of Organic Tethers Bound to MCM41-Type Surfaces from Solid State NMR Measurements. *J. Phys. Chem. C* **2012**, *116* (13), 7442–7449.

(31) Martin, G.J., Martin, M.L., Gouesnard, J.-P. *^{15}N-NMR Spectroscopy*; Springer-Verlag: Berlin, 1981.

(32) Salvatore, R. N.; Yoon, C. H.; Jung, K. W. Synthesis of Secondary Amines. *Tetrahedron* **2001**, *57*, 7785–7811.

(33) Mehring, M. *Principles of High Resolution NMR in Solids*; Springer, 1983.

(34) Gullion, T.; Schaefer, J. Rotational-Echo Double-Resonance NMR. *J. Magn. Reson.* **1989**, *81*, 196–200.

(35) Gullion, T.; Schaefer, J. Detection of Weak Heteronuclear Dipolar Coupling by Rotational-Echo Double-Resonance NMR. In *Advances in Magnetic and Optical Resonance*; 1989; pp 57–84.

(36) Schimming, V.; Hoelger, C.-G.; Buntkowsky, G.; Sack, I.; Fuhrhop, J.-H.; Rocchetti, S.; Limbach, H.-H. Evidence by ^{15}N CPMAS and ^{15}N-^{13}C REDOR NMR for Fixation of Atmospheric CO_2 by Amino Groups of Biopolymers in the Solid State. *J. Am. Chem. Soc.* **1999**, *121*, 4892–4893.

(37) Pinto, M. L.; Mafra, L.; Guil, J. M.; Pires, J.; Rocha, J. Adsorption and Activation of CO_2 by Amine-Modified Nanoporous Materials Studied by Solid-State NMR and $^{13}CO_2$ Adsorption. *Chem. Mater.* **2011**, *23*, 1387–1395.

(38) Li, X.; Hagaman, E.; Tsouris, C.; Lee, J. W. Removal of Carbon Dioxide from Flue Gas by Ammonia\carbonation in the Gas Phase. *Energy Fuels* **2003**, *17*, 69–74.

(39) Jakobsen, J. P.; Krane, J.; Svendsen, H. F. Liquid-Phase Composition Determination in CO_2 - H_2O - Alkanolamine Systems : An NMR Study. *Ind. Eng. Chem. Res.* **2005**, *44*, 9894–9903.

(40) Jarvie, T. P.; Went, G. T.; Mueller, K. T. Simultaneous Multiple Distance Measurements in Peptides via Solid-State NMR. *J. Am. Chem. Soc.* **1996**, *118*, 5330–5331.

(41) Goetz, J. M.; Schaefer, J. REDOR Dephasing by Multiple Spins in the Presence of Molecular Motion. *J. Magn. Reson.* **1997**, *127*, 147–154.

(42) Hahn, M. W.; Steib, M.; Jentys, A.; Lercher, J. A. Mechanism and Kinetics of CO_2 Adsorption on Surface Bonded Amines. *J. Phys. Chem. C* **2015**, *119*, 4126–4135.

(43) Li, K.; Kress, J. D.; Mebane, D. S. The Mechanism of CO_2 Adsorption under Dry and Humid Conditions in Mesoporous Silica-Supported Amine Sorbents. *J. Phys. Chem. C* **2016**, *120*, 23683–23691.

(44) Mafra, L.; Cendak, T.; Schneider, S.; Wiper, P. V.; Pires, J.; Gomes, J. R. B.; Pinto, M. L. Structure of Chemisorbed CO_2 Species in Amine-Functionalized Mesoporous Silicas Studied by Solid-State NMR and Computer Modeling. *J. Am. Chem. Soc.* **2017**, *139*, 389–408.

(45) Choi, S.; Drese, J. H.; Jones, C. W. Adsorbent Materials for Carbon Dioxide Capture from Large Anthropogenic Point Sources. *ChemSusChem* **2009**, *2*, 796–854.

(46) Chang, A. C. C.; Chuang, S. S. C.; Gray, M.; Soong, Y. In-Situ Infrared Study of CO_2 Adsorption on SBA-15 Grafted with Gamma-(Aminopropyl)Triethoxysilane. *Energy & Fuels* **2003**, *17*, 468–473.

(47) Sayari, A.; Belmabkhout, Y.; Da'na, E. CO_2 Deactivation of Supported Amines: Does the Nature of Amine Matter? *Langmuir* **2012**, *28*, 4241–4247.

(48) Sayari, A.; Heydari-Gorji, A.; Yang, Y. CO_2-Induced Degradation of Amine-Containing Adsorbents: Reaction Products and Pathways. *J. Am. Chem. Soc* **2012**, *134*, 13834–13842.

(49) Chen, C.-H.; Shimon, D.; Lee, J. J.; Didas, S. A.; Mehta, A. K.; Sievers, C.; Jones, C. W.; Hayes, S. E. Spectroscopic Characterization of Adsorbed $^{13}CO_2$ on 3-Aminopropylsilyl-Modified SBA15 Mesoporous Silica. *Environ. Sci. Technol.* **2017**, *51*, 6553–6559.

Chapter 3: $^{13}CO_2$ reacted amine-SBA15 in humid conditions

This chapter is based on research described in the following publication.

Title: The "Missing" Bicarbonate in CO_2 Chemisorption Reactions on Solid Amine Sorbents

Authors: Chia-Hsin Chen, Daphna Shimon, Jason J. Lee, Frederic Mentink-Vigier, Ivan Hung, Carsten Sievers, Christopher W. Jones, Sophia E. Hayes

In this chapter, we discuss the unexpected finding of a hydrated bicarbonate formed by chemisorption of $^{13}CO_2$ on aminopropylsilane (APS), methylaminopropylsilane (MAPS), and dimethylaminopropylsilane (DMAPS) pendant molecules grafted on SBA15 mesoporous silica. The most commonly-used sequence in solid-state NMR, ^{13}C CPMAS, failed to detect bicarbonate in these solid amine sorbent samples; therefore, we have employed a Bloch decay ("pulse-acquire") sequence (with ^{1}H decoupling) to detect such species. The water that is present likely contributes to dynamic motion of the bicarbonate product, thwarting CPMAS but enabling direct ^{13}C detection by shortening the spin-lattice relaxation time. Since solid-state NMR plays a major role in characterizing chemisorption reactions, the detection of previously elusive bicarbonate species (which are also challenging to observe in IR spectroscopy)[1] represents an important advance. We note that employing this straightforward NMR technique can reveal the presence of bicarbonate that has often otherwise been overlooked, as demonstrated in APS, that has been thought to only contain adsorbed CO_2 as carbamate and carbamic acid species.[2] As in other systems (e.g, proteins), dynamic species that sample multiple magnetically-inequivalent environments have resonances that tend to broaden as their motion is "frozen out." Here, we

show two distinct bicarbonate species upon cooling to ≈ 100 K, and coupling to different protons is shown through ^{13}C-^{1}H HETCOR measurements. This chapter demonstrates that bicarbonates have likely been formed in the presence of water but have gone unobserved by NMR due to the nature of the experiments most routinely employed, perspective that will transform the way the sorption community will view CO_2 capture by amines, as well as protocols for performing experiments.

3.1 Overview of bicarbonate in humid conditions

The formation of bicarbonate in CO_2 chemisorption reactions on solid amines has been debated in the past.[1,3–6] Solid-state NMR is used extensively to characterize chemisorption products because the method can determine structures of these non-crystalline systems. NMR can be employed in a manner that leads to quantification of products, as well as reactants, and can detect side products that are formed.[7–10] In NMR in particular, the bicarbonate ^{13}C chemical shift appears at a range of values, depending on the environment that contributes to the shielding experienced by the ^{13}C nucleus, and hence is sensitive to pH.[11] As a result, bicarbonate moieties may appear at different frequencies in similar samples, and the NMR resonance may even be masked by that of more prominent carbamate or carbamic acid resonances.[12] Carbonate (CO_3^{2-}) is not observed here, because conditions that favor its formation (pH > 11) are not present. In this work, dimethylaminopropylsilane species (DMAPS) grafted onto SBA15 was selected as an ideal

Scheme 3.1 Proposed reaction of CO_2 with DMAPS in the presence of water.

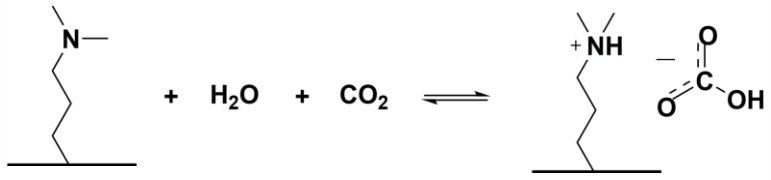

DMAPS bicarbonate

"model" system for characterization by solid-state NMR. (Scheme 3.1) While tertiary amines such as DMAPS are not of practical importance in carbon capture applications due to their low CO_2 uptake,[13] they have been chosen for study here because the only chemisorption product that can be formed is a bicarbonate which requires the presence of water.[14,15] The highly-utilized (and studied) primary and secondary amines (such as APS and MAPS) can adsorb CO_2, forming both carbamate and bicarbonate species.[1,13] For DMAPS there is no obfuscation of the bicarbonate signal with that of carbamate or carbamic acid, which is critical since all three moieties appear in a similar chemical shift region and are therefore very difficult to discriminate from one another.[14,16]

3.2 Experimental section

Sample preparation: Dimethylaminopropylsilane (DMAPS), methylaminopropylsilane (MAPS) and aminopropylsilance (APS) pendant molecules were added to the surface of SBA15 mesoporous silica, forming "solid amine sorbents" (hereafter simply referred to as "DMAPS," "MAPS," and "APS" respectively). These sorbents were each activated though vacuum followed by heating to remove any residual adsorbed gases. Typical procedures were as follows: the sample was placed in a round bottom flask at 105 °C and 40 mTorr vacuum for 4 hours. Subsequently, 40 mg of this activated DMAPS (or MAPS, APS) was mixed with 40 mg water and packed into a zirconia rotor for solid-state NMR. The packed rotor was then put (uncapped) into a glass sample holder, connected to a gas manifold, and then loaded with 1 atm of $^{13}CO_2$ (Sigma-Aldrich, 99% $^{13}CO_2$). Exposure times to this gas ranged from 10 hours to 20 hours after which the rotors were capped and out in sample vials. As reported previously for APS, MAPS, and DMAPS, respectively,[13] surface area for each material was found to be 433, 371, and 418 m^2g^{-1}, pore volume is 0.56, 0.49, and 0.52 cm^3g^{-1}, and nitrogen content is 2.4, 2.5, and 2.1 $mmolNg^{-1}$.

Solid-state NMR: Spectra were examined at multiple solid-state NMR facilities, including labs at Washington University, Department of Chemistry; the National High Magnetic Field Laboratory, Tallahassee, FL; the NMR Laboratory in the Department of Chemistry, Ohio State University facility; and the Georgia Institute of Technology NMR Center.

Room-temperature (RT) experiments: $^{13}C\{^{1}H\}$ MAS and CPMAS spectra of $^{13}CO_2$ reacted APS and MAPS were recorded at 14 T with a Bruker 2.5 mm HX probe operating at ^{13}C frequency of 148.31 MHz and ^{1}H frequency of 589.84 MHz. For $^{13}C\{^{1}H\}$ Bloch decay NMR at room temperature, typical $\pi/2$ pulse widths were 7.5 μs, using a recycle delay of 10 s. For $^{13}C\{^{1}H\}$ CPMAS, the contact time was 2 ms, and a recycle delay of 6 s was used. The MAS rotational frequency was set 10 kHz. $^{13}C\{^{1}H\}$ CPMAS of DMAPS at room temperature was recorded at 7 T with a 5 mm HXY MAS Chemagnetics probe operating at ^{13}C and ^{1}H frequencies of 74.17 MHz and 294.97 MHz, respectively. The contact time was 2 ms, the recycle delay was 4 s, and the MAS rotational frequency was 5 kHz. Data were recorded at Washington University.

Low-temperature (100K) experiments: $^{13}C\{^{1}H\}$ MAS and CPMAS spectra of $^{13}CO_2$ reacted APS, MAPS, and DMAPS were recorded at 14 T with a Bruker 3.2 mm HXY LTMAS probe operating at ^{13}C frequency of 150.93 MHz and ^{1}H frequency of 600.27 MHz. For $^{13}C\{^{1}H\}$ Bloch decay at room temperature and 100 K, the $\pi/2$ pulse width was 4.5 μs, the MAS rotational frequency was 10 kHz, and a recycle delay of 10 s (RT) and 30 s (100K) were used. For $^{13}C\{^{1}H\}$ CPMAS, the contact time was 2 ms, and the recycle delay of 10 s at 100 K. Data were recorded at The Ohio State University NMR facility.

Intermediate-temperature (223K-250K) experiments: $^{13}C\{^{1}H\}$ CPMAS of $^{13}CO_2$-reacted DMAPS at variable temperatures (250 K and 223 K) were recorded at 9.4 T operating at a ^{13}C frequency

of 100.56 MHz and ^{1}H frequency of 399.92 MHz. The contact time was 2 ms, the recycle delay was 4 s, and the MAS rotational frequency was 10 kHz. Data were recorded at the Georgia Institute of Technology facility.

Low-temperature (~97 K) ^{13}C-^{1}H HETCOR experiments: the HETCOR spectrum of $^{13}CO_2$-reacted DMAPS was recorded at 14.1 T with a Bruker 3.2 mm HCN LTMAS probe operating at ^{13}C frequency of 150.89 MHz and ^{1}H frequency of 600.11 MHz. The $^{13}C\{^{1}H\}$ CPMAS contact time was set to 150 μs, and a proton decoupling power of 100 kHz. The spinning speed was set to 7 kHz, and the recycle delay was optimized and set to 19.5 s. The HETCOR spectrum was obtained with 64 points in the indirect dimension while applying supercycled PMLG5$^{\bar{x}x}_{mm}$ homonuclear decoupling[17,18], optimized as detailed in Ref [19]. The scaling factor (s = 0.59) and proton chemical shift were obtained by applying the sequence under the same conditions to a solid-state glycine sample. Data were recorded at National High Magnetic Field Laboratory.

3.3 ^{13}C NMR of $^{13}CO_2$ reacted wet DMAPS

Figure 3.1 shows $^{13}C\{^{1}H\}$ NMR spectra for $^{13}CO_2$-reacted DMAPS that was dampened substantially with water prior to $^{13}CO_2$ gas exposure. Figure 3.1a is the result of a room temperature ("RT") Bloch decay magic-angle spinning (MAS) NMR experiment and shows a very narrow (for solid-state NMR) 270 Hz ^{13}C resonance centered at 163 ppm (experiments with and without ^{1}H decoupling were identical; here, ^{1}H decoupling is included for all experiments for consistency). Figure 3.1b is a $^{13}C\{^{1}H\}$ CPMAS spectrum at RT and shows that no signal is observed. (Note: a very small signal can be observed on occasion, with no discernable correlation to experimental conditions, simply reflective of better or poorer Hartmann-Hahn matching). Below, are two low-temperature 100 K NMR experiments: Figure 3.1c is $^{13}C\{^{1}H\}$ Bloch decay MAS NMR, and Figure

3.1d is a $^{13}C\{^{1}H\}$ CPMAS experiment. In both, the single room-temperature resonance is separated into two species, which are broadened considerably and shifted from that of the bicarbonate signal

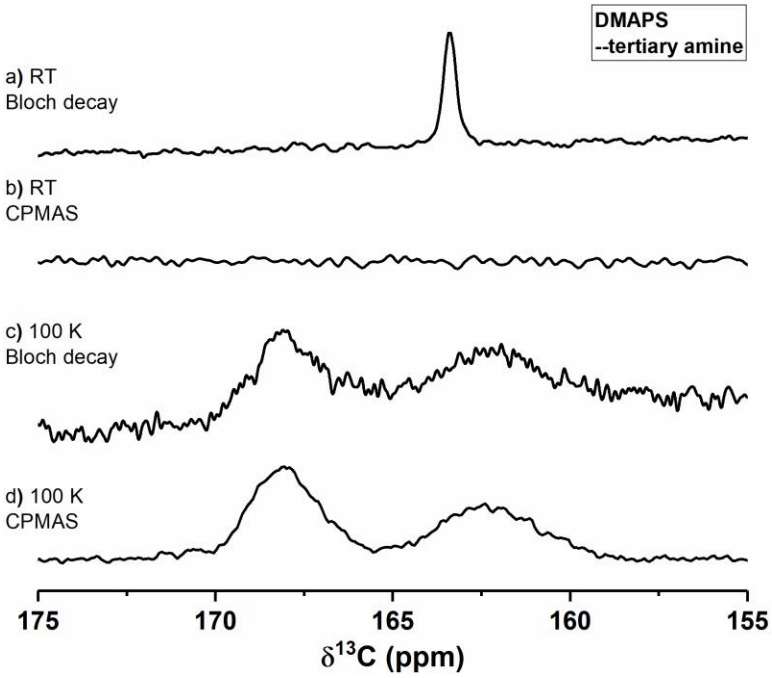

Figure 3.1 Bicarbonate ^{13}C NMR from CO_2-reacted DMAPS-SBA15: a) and b) at room temperature (RT) via $^{13}C\{^{1}H\}$ MAS Bloch decay NMR ("pulse-acquire"), and $^{13}C\{^{1}H\}$ CPMAS, respectively; c) and d) at 100 K by the same sequences, as indicated on the figure. Rotational frequency for MAS, ν_r, was 10 kHz.

at RT. The similarity of appearance between the two spectra shows that both are in hydrogen-rich sites, where a better signal-to-noise ratio is obtained with CP.

What is significant is that the low temperature experiment shows that $^{13}C\{^{1}H\}$ CPMAS is now feasible under low temperature conditions, even though it "failed" at room temperature. With dynamic motion arrested, cross-polarization is possible, suggesting that dynamic averaging occurs in highly hydrated samples at RT. Upon freezing, there is an induced speciation into two magnetically-inequivalent sites. We find that the Figure 3.1 observations can be "cycled" between

low and high temperatures, and the speciation is reversible. That is, when the sample is warmed, a single resonance is observed again at room temperature. We surmise that one of the two signals is hydrated bicarbonate, but now "motionally-arrested", thereby permitting efficient ^{1}H-^{13}C dipole-dipole coupling. The other resonance is slightly more challenging to assign. The two species are shifted in frequency from one another, indicating these are different chemical environments; however, both species are assigned as bicarbonate, as other forms of chemisorbed CO_2 on tertiary amines (i.e., carbamate, carbamic acid) are not expected. Carbonate (CO_3^{2-}) is a possibility in highly basic environments; however, this species has not been found in these solid amine systems (but cannot be conclusively ruled out.) In order to determine the chemical identity of the second species, we look to the example of a related system: $^{15}N\{^{1}H\}$ CPMAS of pyridine in SBA15 at 120 K to 130 K.[22,23] by Buntkowsky and co-workers. In this work, two pyridine signals were observed by ^{15}N NMR, assigned to a surface-bound species, and a "free" pyridine. At room

temperature, one pyridine resonance was observed. Another example is the study of dipeptide adsorbed SBA15 by Jayanthi et al., two different characteristic adsorbate sites were identified—a so-called "frozen" conformation arising from interactions with the surface, and one where the adsorbate adopts an "isotropic-like motional state."[24,25] We have examined a series of spectra over temperatures ranging from 100 K to room temperature. The narrow bicarbonate resonance at 250 K broadens and shifts slightly to high frequency at 223 K, and a second resonance is evident as a small shoulder, denoted by an arrow in Figure 3.2. Figure 3.2 shows the beginning of evident for two-site exchange between these resonances, where the NMR signals arise as a weighted average between two sites, with a "coalescence region" in between. Such exchange phenomena have also been observed in a dipeptide of glycine-(2,2)-d_2-alanine adsorbed on SBA15 in the presence of minimal amounts of water,[24] at 4 to 7 H_2O molecules/nm^2.

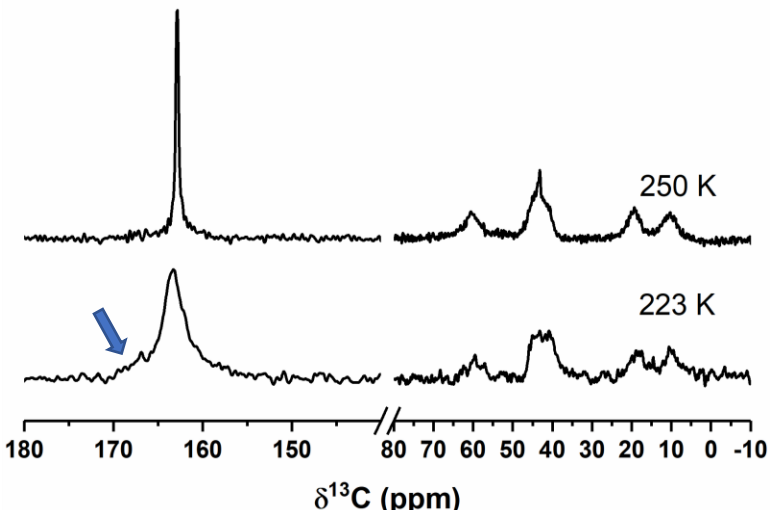

Figure 3.2 Variable temperature $^{13}C\{^1H\}$ CPMAS from water-dampened $^{13}CO_2$- reacted DMAPS solid-amine sorbent at 250 K and 223 K. The enriched bicarbonate signal(s) appear in the region from 160-170 ppm; the sp^3 carbons (at natural abundance) on the dimethylaminopropyl pendant species are shown in the region from 5 to 65 ppm.

In an attempt to further characterize the two sites, ^{13}C-^{1}H HETCOR at low temperature (100 K) was performed. Figure 3.3(a) shows a 2-dimensional ^{13}C-^{1}H HETCOR plot that shows the two bicarbonate signals at low temperatures are coupled to different protons, leading to their chemical- and magnetic-inequivalence. The ^{13}C resonance at 162 ppm has cross-peaks with two proton environments, at 3.5 ppm and 5.5 ppm for ^{1}H. The ^{13}C resonance at 168 ppm has only one cross-peak at $^{1}H \approx 4$ ppm, which is consistent with the proton chemical shift of "physisorbed" water.[26] Xu et al. used *in situ* solid-state NMR to monitor the adsorption of water in porous silica and found multiple water environments including adsorbed water (interacting, hydrogent-bonded, with the surface hydroxide) at ^{1}H 5.4 ppm and another physisorbed water environment at ^{1}H 3.8 ppm that does not couple to the surface. We surmise that the 168 ppm resonance couples to the water that is not hydrogen-bonded to the surface, such as a hydrated bicarbonate in the "middle" of the SBA15 pore structure. The 162 ppm resonance couples to another water environment,[26] that we describe using the rest of the HETCOR plot.

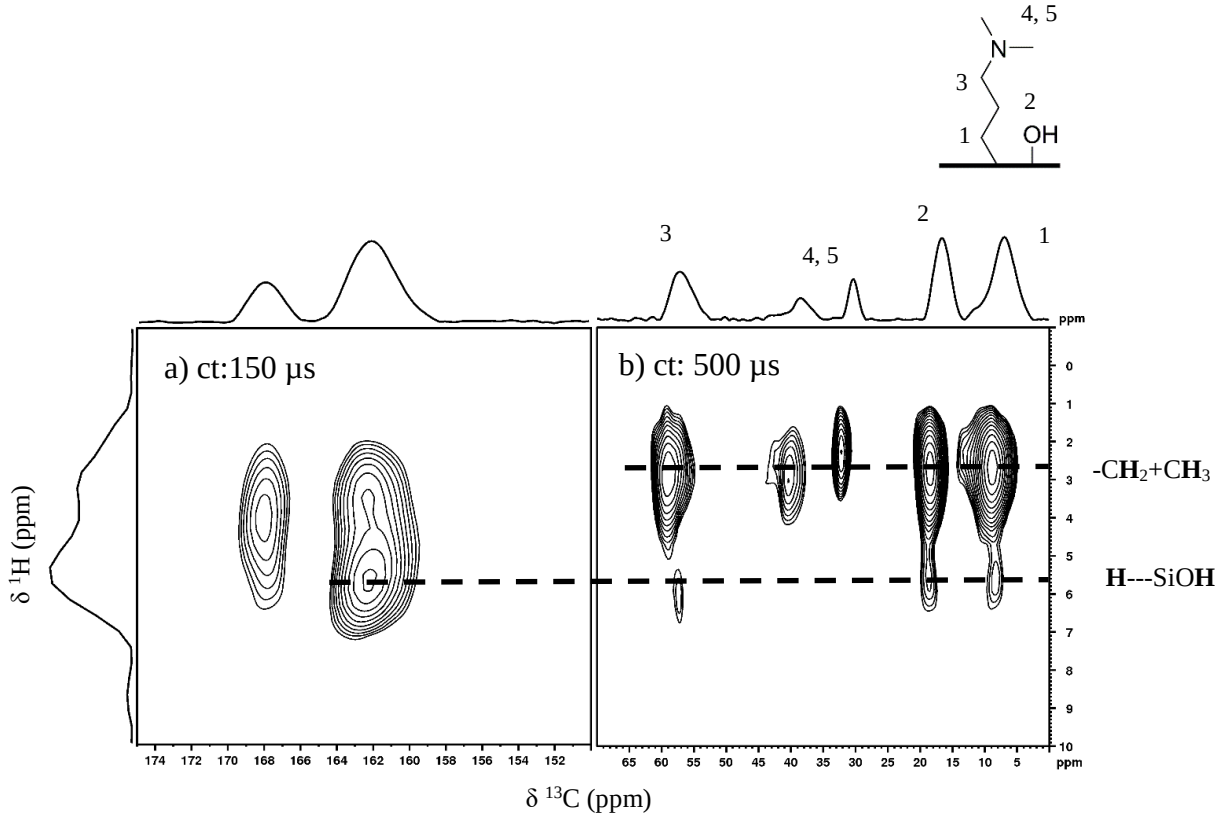

Figure 3.3 ^{13}C-^{1}H HETCOR of bicarbonate from $^{13}CO_2$ reacted DMPAS-SBA15 at 100 K. (a) carbonyl carbon region at contact time of 150 µs and (b) aliphatic carbon region at contact time of 500 µs. The dash line at 2.5 ppm is assigned to C**H**$_2$ and C**H**$_3$ and the dash line at 5.5 ppm is assigned to the H-bonded surface hydroxide.

Figure 3.3(b) shows the aliphatic carbon region and the assignments of carbon in pendant DMAPS. These *sp*^{3} carbons in DMPAS have cross-peaks with a ^{1}H chemical shift at ≈ 2.5 ppm, the protons of methyl and methylene groups. Carbon 1, 2, and 3 in a DMAPS have another cross-peak with the ^{1}H ≈ 5.5 ppm resonance, noting this correlation is <u>weak</u> and does not appear at short contact times. The ^{1}H ≈ 5.5 ppm chemical shift is consistent with the proton chemical shift of surface Si-OH hydroxide which is hydrogen bonded to water.[9,26–29] This correlation suggests that the carbon backbone of DMAPS couples to the surface hydroxide, and the more distant carbons 4 and 5 do not show any coupling. One possibility for why carbons 4 and 5 do not show any

correlation to ^{1}H at 5.5 ppm could be due to motional averaging from slow methyl rotation (averaging all ^{13}C-^{1}H couplings but the directly-bonded ^{13}C-^{1}H interaction). Notably, the ^{13}C resonance at 162 ppm has a cross-peak to this ^{1}H ≈5.5 ppm proton which suggests that this bicarbonate is also close to the surface hydroxide. A proposed model of two bicarbonates is dipicted in Scheme 3.2, where the two bicarbonates couple to different water environments. The ^{13}C 168 ppm resonance is surrounded by water and is distant from the surface, and the ^{13}C 162 ppm species is coupled to surface adsorbed water at Si-OH sites and the protons from water at 3.5 ppm that are not hydrogen-bonded to the surface.

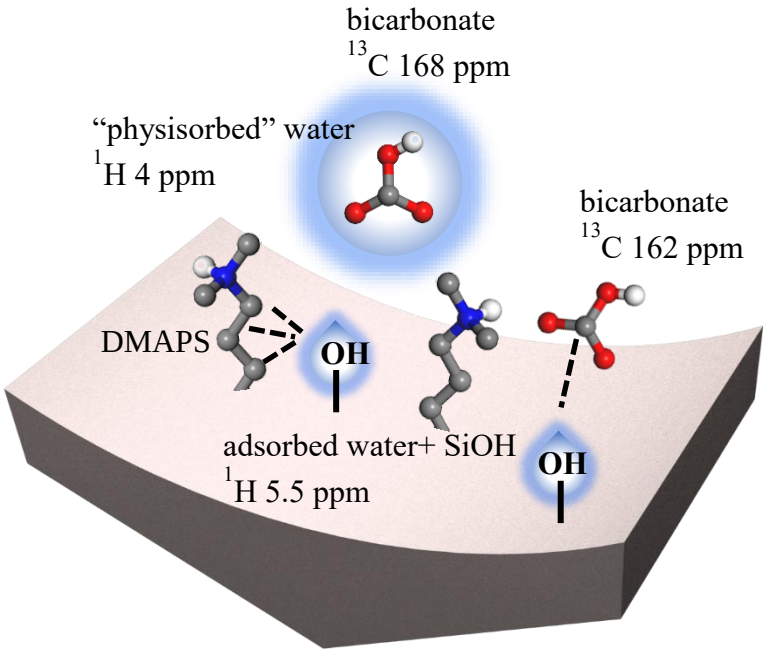

Scheme 3.2 A proposed model of pendant DMAPS on a pore surface of SBA15 mesoporous silica. Water on the silica indicated by "droplet" shapes ("–OH), and water hydrating bicarbonate away from the surface is the shaded blue sphere. Two bicarbonates from water-damped, $^{13}CO_2$ –reacted DMAPS-SBA15 at 100 K. The dotted line represents coupling.

3.4 ^{13}C NMR of $^{13}CO_2$ reacted wet DMAPS (D_2O exposure)

We probe further this model of two bicarbonate ^{13}C signals at 100 K, one close to surface and another further away from the surface surrounded by physisorbed water as detailed in section 3.3. To examine this model, we use D_2O in place of H_2O to facilitate the reaction of DMAPS and $^{13}CO_2$ to form both deuterated bicarbonate and its hydration. In theory, only the bicarbonate signal that is coupled to the surface hydroxides (that still possess their 1H's) will show in $^{13}C\{^1H\}$ CPMAS. The other bicarbonate, surrounded by D_2O, will not show up in $^{13}C\{^1H\}$ CPMAS because there is no ^{13}C-^1H dipolar interaction present. $^{13}C\{^1H\}$ CPMAS of D_2O wetted $^{13}CO_2$ reacted DMAPS is shown in Figure 3.4. The red line represents $^{13}C\{^1H\}$ bicarbonate spectrum formed when using H_2O, and the black line represents bicarbonate formed using D_2O. There are still two resonances

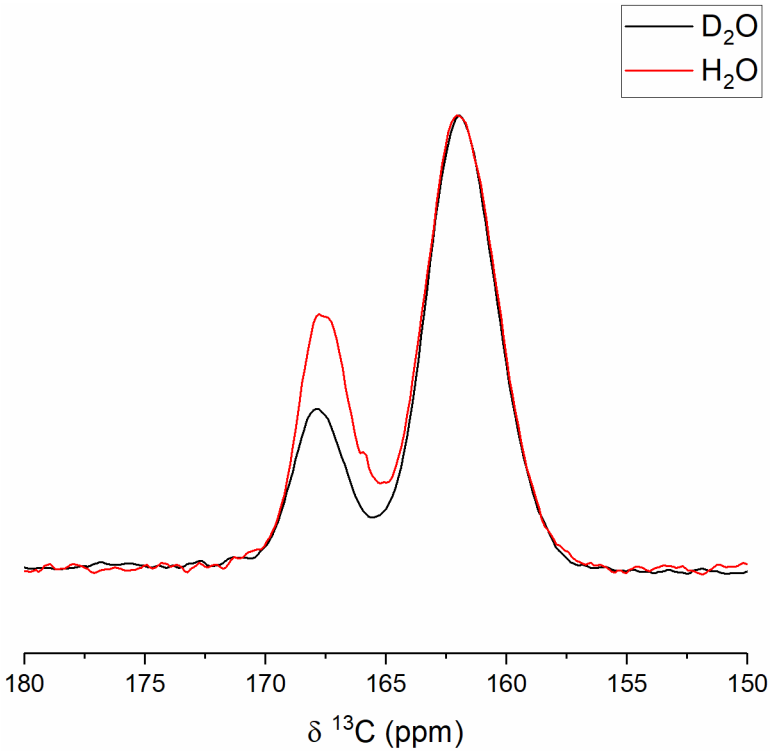

Figure 3.4 $^{13}C\{^1H\}$ CPMAS of $^{13}CO_2$ reacted DMAPS-SBA15 at 100 K. Black line represents bicarbonate formed from H_2O exposure and red line represents bicarbonate formed from D_2O exposure.

in the D_2O-exposed DMAPS, and the 168 ppm resonance is attenuated with D_2O uses. It is possible that the surface hydroxide protons are exchangeable; so, a small amount of D_2O exchanges with the surface hydroxide and becomes mostly HDO. The ^{13}C 168 ppm bicarbonate now is surround by D_2O, HDO, and possibly some H_2O, which results in an attenuated CP signal compared to the H_2O-exposed experiment. Figure 3.5 shows ^{13}C-^{1}H HETCOR of $^{13}CO_2$ reacted wet DMAPS (D_2O exposed) at 100 K. Five ^{13}C resonances at 0-60 ppm are assigned to the aliphatic carbons in pendant DMAPS (referred to Figure 3.3) with protons still present on the sp^3 carbons. They have similar cross-peaks with ^{1}H at 3.3 ppm, which are protons of methyl/methylene. The two ^{13}C resonances of bicarbonate in Figure 3.5 show more complex correlations but better resolution than the HETCOR of Figure 3.3. Figure 3.3 resonances were not as resolvable because of the strong homonuclear dipolar interactions due to a large amount of H_2O wetting the samples. The two bicarbonates have new cross-peaks in Figure 3.5. By using D_2O to react with DMAPS and form bicarbonate, it reduces the strong ^{1}H-^{1}H dipolar interaction and reveals new cross-peaks. Both ^{13}C resonances at 162 and 168 ppm couple to protons at 3.3 ppm, which is the H's the carbon backbone of pendant DMAPS. The coupling of the two bicarbonates to the pendant DMAPS is consistent with our proposed reaction in Scheme 3.1, with additional caveat– that both bicarbonates are in proximity with neighboring pendant DMAPS but with the 162 ppm resonance in a distinct (now-resolved) environment. The different proton environments lead to two ^{13}C chemical shifts of bicarbonate: the 162 ppm resonance corresponds to the bicarbonate that is close to the surface hydroxide, further coupled to adsorbed water and the sp^3 carbons. 168 ppm resonance corresponds to the bicarbonate that is far away from surface and coupled to the physisorbed water, but also in proximity to the sp^3 carbons to allow for dipole-dipole interactions to these.

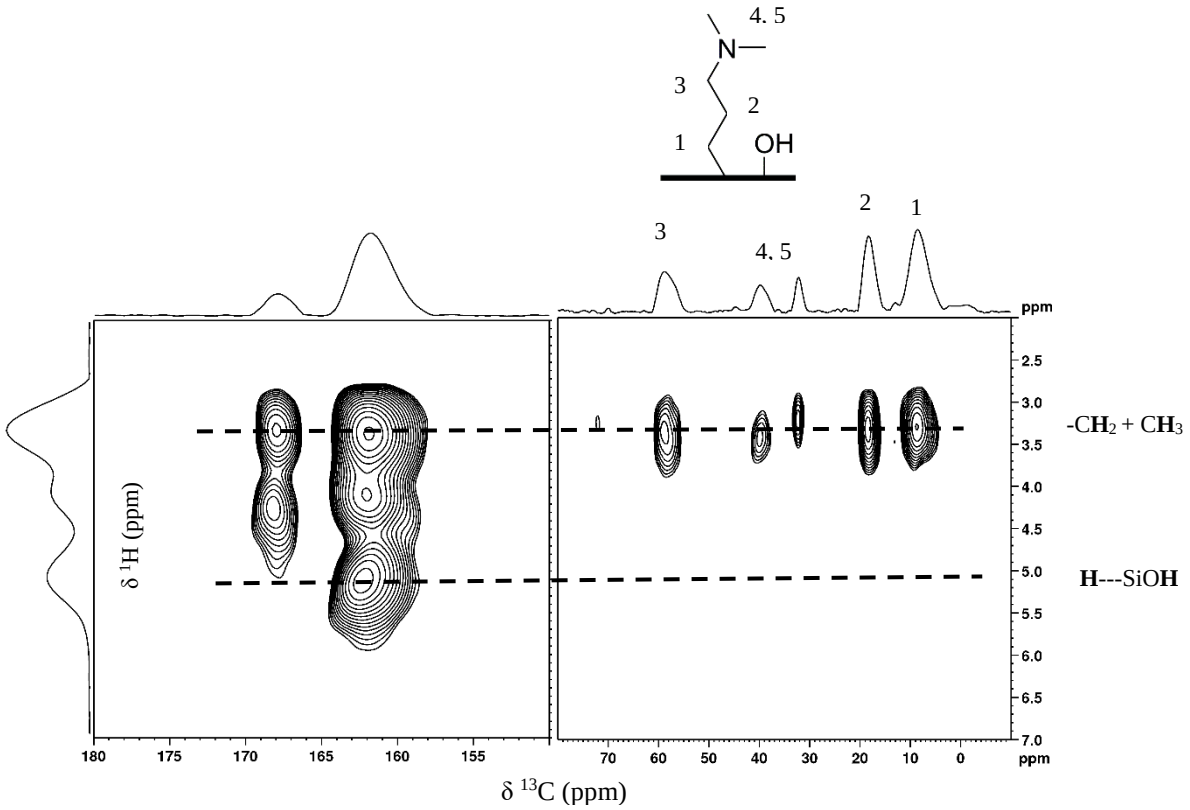

Figure 3.5 ^{13}C-^{1}H HETCOR of bicarbonate from D_2O exposed $^{13}CO_2$ reacted DMAPS-SBA15at 100 K. The dashed line at 3.3 ppm is assigned to C**H**$_2$ and C**H**$_3$ and the dashed line at 5.5 ppm is assigned to the H-bonded surface hydroxide.

3.5 $^{13}CO_2$ reacted APS and MAPS

Aminopropylsilnae (APS) and methylaminopropylsilane (MAPS) are two other relevant pendant species that with H_2O present react with CO_2 and form chemisorbed products species, which can be carbamate, and bicarbonate (Scheme 3.3). (More details can be referred to Chapter 2). To demonstrate the generality of the presence of bicarbonate in other pendant amine systems, in Figure 3.6 we show a pair of ^{13}C solid-state NMR spectra for a related $^{13}CO_2$-reacted primary amine pendant molecule, aminopropylsilane (APS), in SBA15. Adsorbents containing these functional groups have been widely studied by ^{13}C NMR after exposure to $^{13}CO_2$.[2,16] Again, in the presence of water, using $^{13}C\{^1H\}$ MAS Bloch decay, we observe both a bicarbonate signal (at 161 ppm) and a second signal that we have assigned previously[16] at 164 ppm to carbamate (Figure 3.6a). Also, notable in the $^{13}C\{^1H\}$ CPMAS spectrum shown in Figure 3.6b is a tiny signal attributable to bicarbonate. Substantial motional averaging of bicarbonate decreases the intensity of this signal when relying on dipole-dipole coupling between ^1H and ^{13}C spins in CPMAS, hence the signal is challenging to record when relying cross-polarization. Figure 3.7 shows the ^{13}C NMR of $^{13}CO_2$ reacted secondary amine methylaminopropylsilane, (MAPS)-

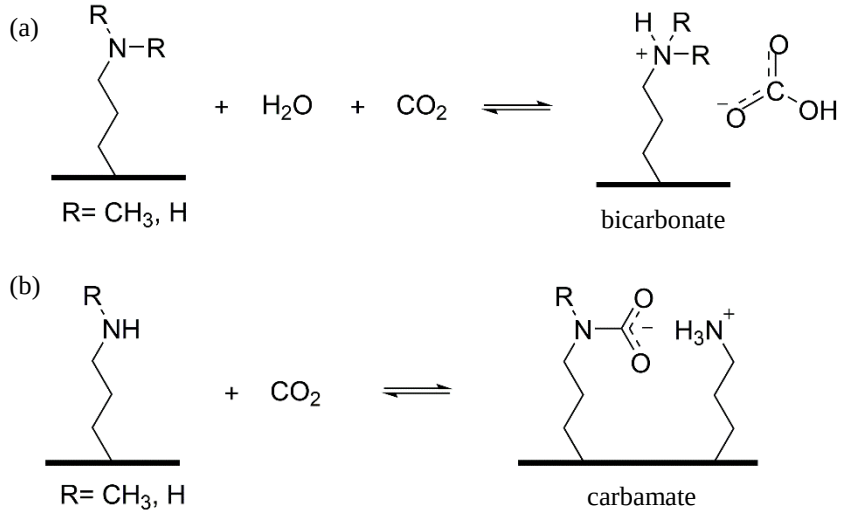

Scheme 3.3 Proposed reaction of CO_2 with a primary amine and a secondary amine.

SBA15. The ^{13}C resonance at 164 ppm is assigned to carbamate (see chapter 2) The 161 ppm resonance also shows the same chemical shift as bicarbonate in APS and DMAPS, and an attenuated CP signal due to motional averaging, which we assign to bicarbonate.

We have shown that bicarbonate is able to be formed in three types of amines: primary, secondary and tertiary. As shown and discussed in Section 3.3, bicarbonate turns into two distinct ^{13}C resonances when cooled to 100 K: 168 ppm, which we assign to the bicarbonate coupled to "interior" water which does not couple to the surface, and 162 ppm, which is the bicarbonate that couples to the surface-adsorbed water. Figure 3.9 is the $^{13}C\{^{1}H\}$ CPMAS of $^{13}CO_2$ reacted wet APS, MAPS, and DMAPS at 100 K where carbamate at 164 ppm and the two bicarbonate resonances may all be present. The two bicarbonate signals are also found in the primary and secondary amines, APS and MAPS.

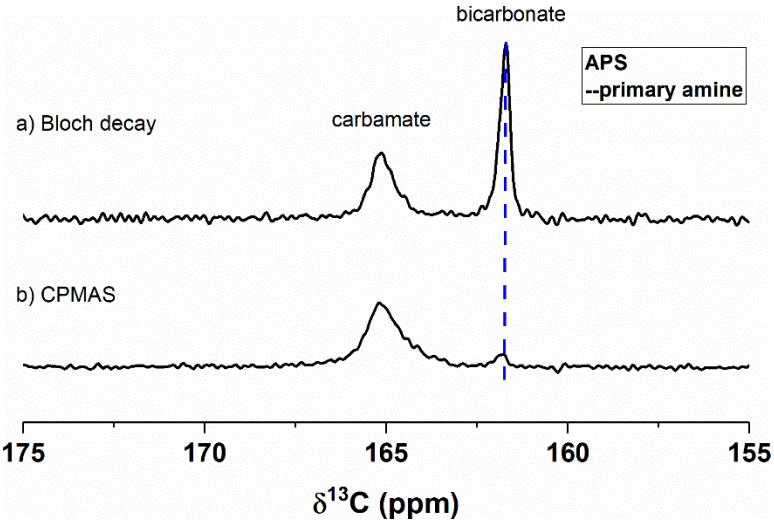

Figure 3.6 $^{13}CO_2$- reacted water-dampened aminopropylsilane (APS)-SBA15 solid-amine sorbent forms both carbamate and bicarbonate, evidenced by ^{13}C NMR at room temperature: a) via $^{13}C\{^1H\}$ MAS Bloch decay, and b) via $^{13}C\{^1H\}$ CPMAS.

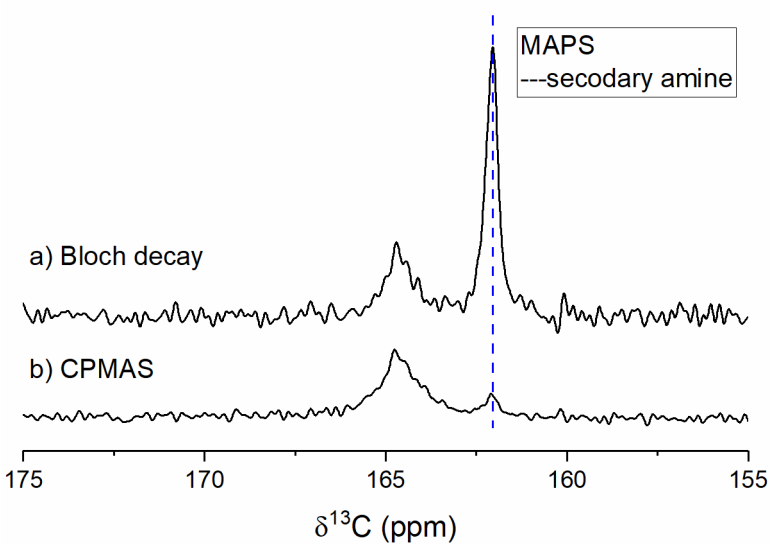

Figure 3.7 $^{13}CO_2$- reacted water dampened methylaminopropylsilane (MAPS)-SBA15 solid-amine sorbent forms both carbamate and bicarbonate, evidenced by ^{13}C NMR at room temperature: a) via $^{13}C\{^1H\}$ MAS Bloch decay, and b) via $^{13}C\{^1H\}$ CPMAS.

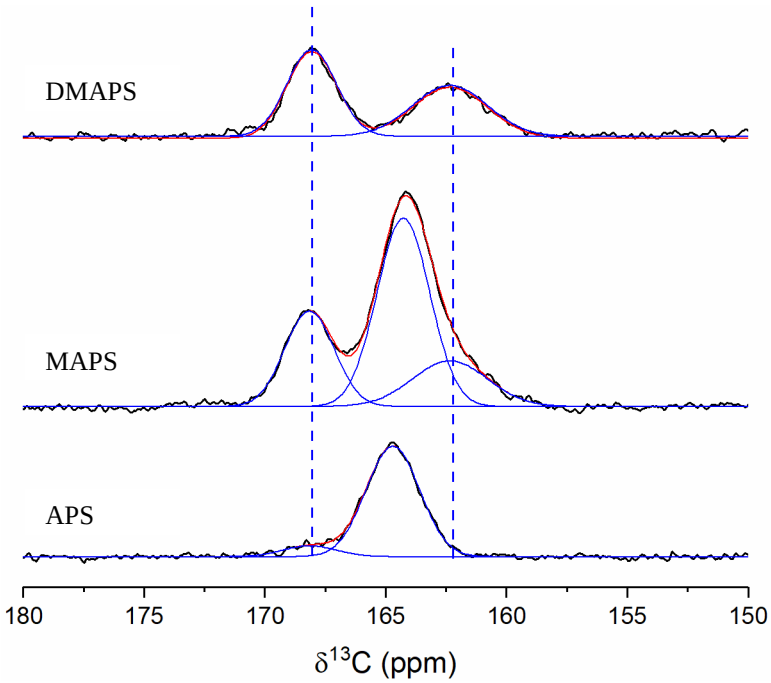

Figure 3.8 $^{13}C\{^{1}H\}$ CPMAS of water-dampened $^{13}CO_2$ reacted solid amine sorbents at 100 K. Top is DMAPS (3° amine), middle is MAPS (2° amine) and the bottom is APS (1° amine). The dashed line at 168 and 162 ppm represents the two bicarbonate signals. The blue line represents the peak deconvolution, red represents the sum of fitted peaks, and black represents experimental data.

3.6 Test of water confinement effects

Mesoporous silica has a high surface area and contains pores and channels of similar sizes resulting in a variety of applications such as catalysis, drug delivery, and gas storage.[30] To increase the efficiency of these applications, it is critical to consider host-guest interactions and the thermodynamic changes of confined guest molecules. It is not known if guest molecules confined in nanoscale pores of solid-amine sorbents show different properties from those in the bulk.[31] Examples of confined molecules changing properties include the decreased of the melting point of confined water by ~ 50 K (273 K to 223 K) and liquid-like of behavior of confined solid-state ibuprofen.[31–33] The binding strength to the inner surface of mesoporous silica can determine the dynamic properties of confined guest molecules. It has been reported in mesoporous silica that as few as 4-7 water molecules per nm^2 can induce local motion of bound guest molecules on the silica surface.[24]

In the water-dampened $^{13}CO_2$ reacted amine-SBA15, hydrated bicarbonate shows liquid-like behavior which leads to inefficient CPMAS. It brings up a question: what causes the dynamic motion of bicarbonate? Is the dynamic motion induced by the surrounding water, or is the bicarbonate in a confined environment and adopting liquid-like behavior? To examine if the confinement induces the dynamic motion of bicarbonate, we used microsopic SiO_2 particles (Cabosil, fumed silica) as the amine support instead of SBA15 (a porous silica.) Figure 3.10 shows the ^{13}C NMR of water-dampened $^{13}CO_2$ reacted APS-Cabosil. Using a Bloch decay, we observe two resonances at 164 ppm and 161 ppm. The 164 ppm resonance is assigned to carbamate, and the ^{13}C 161 ppm resonance is assigned to bicarbonate (see Section 3.5.) The bicarbonate shows dynamic motion on high surface area fumed silica and has an attenuated CP signal, suggesting that the dynamic motion is not induced by confinement since this is not a

mesoporous material. Figure 3.11 shows the ^{13}C NMR of $^{13}CO_2$ reacted DMAPS-Cabosil. The only chemisorbed product of DMAPS (a tertiary amine) that can be formed is bicarbonate (Scheme 3.1), and again, bicarbonate is found on this high surface area fumed silica with amine pendants, not requiring nano-confinement for motional narrowing. The ^{13}C 161 ppm resonance is assigned to bicarbonate and in exhibiting dynamic behavior causing inefficient CP.

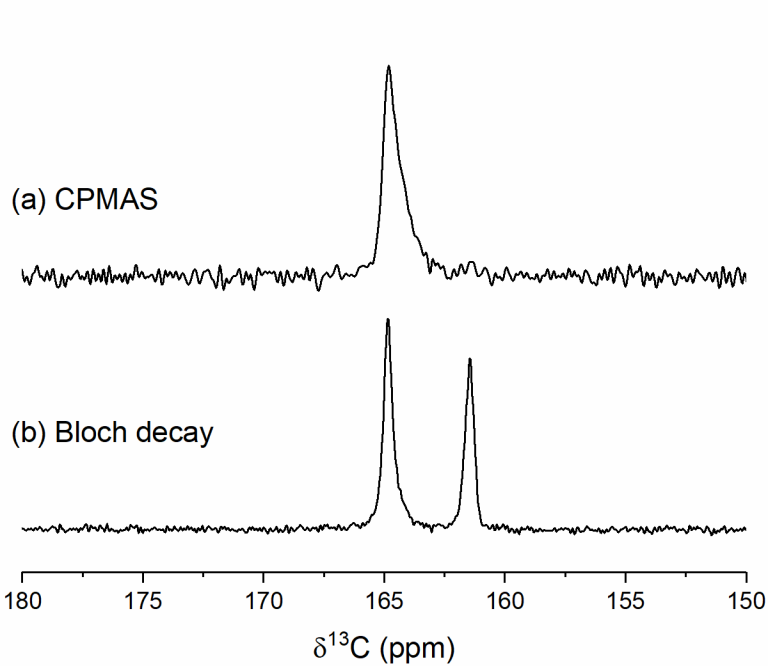

Figure 3.9 Water-dampened and $^{13}CO_2$- reacted aminopropylsilane (APS)-Cabosil, solid-amine sorbent forms both carbamate and bicarbonate, evidenced by ^{13}C NMR at room temperature: (a) via $^{13}C\{^1H\}$ CPMAS, and (b) via $^{13}C\{^1H\}$ MAS Bloch decay.

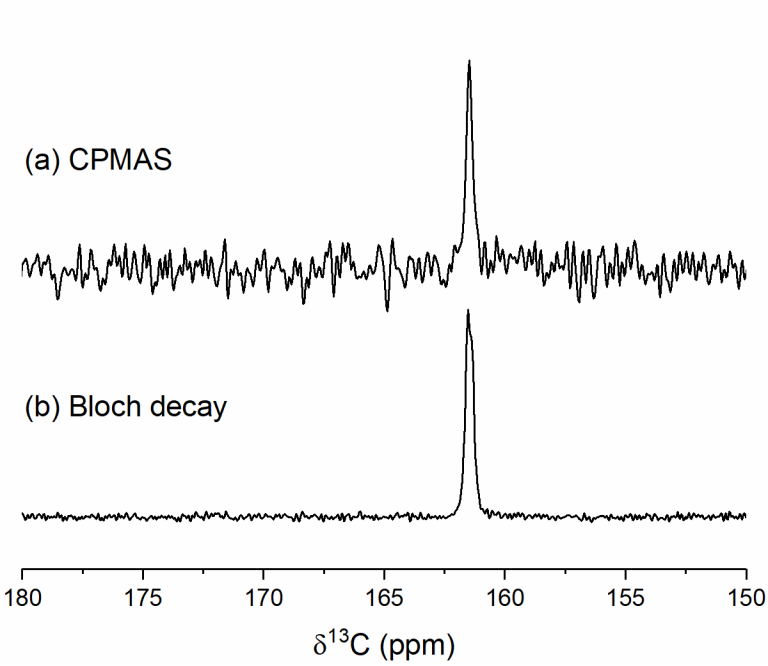

Figure 3.10 Water-dampened and $^{13}CO_2$- reacted dimethylaminopropylsilane (DMAPS)-Cabosil form bicarbonate evidenced in ^{13}C NMR at room temperature: (a) via $^{13}C\{^1H\}$ CPMAS, and (b) via $^{13}C\{^1H\}$ MAS Bloch decay.

3.7 Conclusion

Using conventional NMR data collection procedures at room temperature, the bicarbonate ^{13}C signal is significantly attenuated—or absent ;therefore, the chemisorption products may potentially be missed or "mis-assigned" inadvertently by using this standard technique. Because Bloch decay is so infrequently successful, owing to the long ^{13}C T_1 relaxation times that are typically found in solids, it is a sequence that is not often employed. Thus, these ^{13}C NMR data show how researchers might have overlooked important chemisorbed products, and it is imperative that both CPMAS and MAS Bloch decay sequences be applied to study these CO_2 capture reactions in solid amine sorbents in the future.

In summary, a single narrow resonance at 163 ppm observed in $^{13}C\{^1H\}$ Bloch decay NMR of DMAPS, MAPS and APS grafted onto mesoporous silica, is assigned to bicarbonate. We show in this work, to our surprise, that bicarbonates have likely been present all along under humid conditions, but they may have been missed by solid-state NMR. We selected DMAPS, a tertiary amine adsorbent, to identify the adsorbed product—bicarbonate--but then extended the metholodology to show that the same species also form on primary and secondary amine-containing samples. CPMAS of hydrated-bicarbonate formed from DMAPS is only consistently possible at very low temperatures, because this species shows dynamic motion caused by surrounding water.[13,14] The motion is arrested at 100 K, where bicarbonate then appears as two chemically-distinct species: one that retains a hydrated "shell", and one is associated with the surface of the solid-amine sorbent. The two-site exchange model between bicarbonate surrounded by water and surface-bound bicarbonate at intermediate (223 K and higher) is consistent with other literature precedent and our data. Therefore, researchers exploring CO_2 adsorption in materials are

cautioned to perform both Bloch decay and $^{13}C\{^{1}H\}$ CPMAS in order to examine the possible existence of bicarbonate.

References (Chapter 3)

(1) Didas, S. A.; Sakwa-novak, M. A.; Foo, G. S.; Sievers, C.; Jones, C. W. Effect of Amine Surface Coverage on the Co-Adsorption of CO_2 and Water: Spectral Deconvolution of Adsorbed Species. *J. Phys. Chem. Lett.* **2014**, *5*, 4194–4200.

(2) Pinto, M. L.; Mafra, L.; Guil, J. M.; Pires, J.; Rocha, J. Adsorption and Activation of CO_2 by Amine-Modified Nanoporous Materials Studied by Solid-State NMR and $^{13}CO_2$ Adsorption. *Chem. Mater.* **2011**, *23*, 1387–1395.

(3) Wang, X.; Schwartz, V.; Clark, J. C.; Ma, X.; Overbury, S. H.; Xu, X.; Song, C. Infrared Study of CO_2 Sorption over "Molecular Basket" Sorbent Consisting of Polyethylenimine-Modified Mesoporous Molecular Sieve. *J. Phys. Chem. C* **2009**, *113*, 7260–7268.

(4) Bacsik, Z.; Ahlsten, N.; Ziadi, A.; Zhao, G. Y.; Garcia-Bennett, A. E.; Martín-Matute, B.; Hedin, N. Mechanisms and Kinetics for Sorption of CO_2 on Bicontinuous Mesoporous Silica Modified with n-Propylamine. *Langmuir* **2011**, *27*, 11118–11128.

(5) Hahn, M. W.; Steib, M.; Jentys, A.; Lercher, J. A. Mechanism and Kinetics of CO_2 Adsorption on Surface Bonded Amines. *J. Phys. Chem. C* **2015**, *119*, 4126–4135.

(6) Moore, J. K.; Sakwa-Novak, M. A.; Chaikittisilp, W.; Mehta, A. K.; Conradi, M. S.; Jones, C. W.; Hayes, S. E. Characterization of a Mixture of CO_2 Adsorption Products in Hyperbranched Aminosilica Adsorbents by ^{13}C Solid-State NMR. *Environ. Sci. Technol.* **2015**, *49*, 13684–13691.

(7) Bernin, D.; Hedin, N. Perspectives on NMR Studies of CO_2 Adsorption. *Curr. Opin. Colloid Interface Sci.* **2018**, *33*, 53–62.

(8) Flaig, R. W.; Osborn Popp, T. M.; Fracaroli, A. M.; Kapustin, E. A.; Kalmutzki, M. J.; Altamimi, R. M.; Fathieh, F.; Reimer, J. A.; Yaghi, O. M. The Chemistry of CO_2 Capture

in an Amine-Functionalized Metal-Organic Framework under Dry and Humid Conditions. *J. Am. Chem. Soc.* **2017**, *139*, 12125–12128.

(9) Hung, C.-T.; Yang, C.-F.; Lin, J.-S.; Huang, S.-J.; Chang, Y.-C.; Liu, S.-B. Capture of Carbon Dioxide by Polyamine-Immobilized Mesostructured Silica: A Solid-State NMR Study. *Micropouous mesoporous Mater.* **2017**, *238*, 2–13.

(10) Andreoli, E.; Dillon, E. P.; Cullum, L.; Alemany, L. B.; Barron, A. R. Cross-Linking Amine-Rich Compounds into High Performing Selective CO_2 Absorbents. *Sci. Rep.* **2014**, *4*, 7304.

(11) Mani, F.; Peruzzini, M.; Stoppioni, P. CO_2 Absorption by Aqueous NH_3 Solutions : Speciation of Ammonium Carbamate , Bicarbonate and Carbonate by a ^{13}C NMR Study. *Green Chmiestry* **2006**, *8*, 995–1000.

(12) Li, X.; Hagaman, E.; Tsouris, C.; Lee, J. W. Removal of Carbon Dioxide from Flue Gas by Ammonia\carbonation in the Gas Phase. *Energy Fuels* **2003**, *17*, 69–74.

(13) Foo, G. S.; Lee, J. J.; Chen, C.-H.; Hayes, S. E.; Sievers, C.; Jones, C. W. Elucidation of Surface Species through in Situ FTIR Spectroscopy of Carbon Dioxide Adsorption on Amine-Grafted SBA-15. *ChemSusChem* **2017**, *10*, 266–276.

(14) Lee, J. J.; Chen, C.-H.; Shimon, D.; Hayes, S. E.; Sievers, C.; Jones, C. W. Effect of Humidity on the CO_2 Adsorption of Tertiary Amine Grafted SBA-15. *J. Phys. Chem. C* **2017**, *121*, 23480–23487.

(15) Lee, J. J.; Yoo, C.-J.; Chen, C.-H.; Hayes, S. E.; Sievers, C.; Jones, C. W. Silica-Supported Sterically Hindered Amines for CO_2 Capture. *Langmuir* **2018**, *34*, 12279–12292.

(16) Chen, C.-H.; Shimon, D.; Lee, J. J.; Didas, S. A.; Mehta, A. K.; Sievers, C.; Jones, C. W.;

Hayes, S. E. Spectroscopic Characterization of Adsorbed $^{13}CO_2$ on 3-Aminopropylsilyl-Modified SBA15 Mesoporous Silica. *Environ. Sci. Technol.* **2017**, *51*, 6553–6559.

(17) Leskes, M.; Madhu, P. K.; Vega, S. A Broad-Banded z-Rotation Windowed Phase-Modulated Lee-Goldburg Pulse Sequence for ^{1}H Spectroscopy in Solid-State NMR. *Chem. Phys. Lett.* **2007**, *447*, 370–374.

(18) Leskes, M.; Madhu, P. K.; Vega, S. Supercycled Homonuclear Dipolar Decoupling in Solid-State NMR: Toward Cleaner ^{1}H Spectrum and Higher Spinning Rates. *J. Chem. Phys.* **2008**, *128*, 052309-11.

(19) Mao, K.; Pruski, M. Homonuclear Dipolar Decoupling under Fast MAS: Resolution Patterns and Simple Optimization Strategy. *J. Magn. Reson.* **2010**, *203*, 144–149.

(20) Akiva-Tal, A.; Kababya, S.; Balazs, Y. S.; Glazer, L.; Berman, A.; Sagi, A.; Schmidt, A. In Situ Molecular NMR Picture of Bioavailable Calcium Stabilized as Amorphous $CaCO_3$ Biomineral in Crayfish Gastroliths. *Proc. Natl. Acad. Sci.* **2011**, *108*, 14763–14768.

(21) Ben Shir, I.; Kababya, S.; Katz, I.; Pokroy, B.; Schmidt, A. Exposed and Buried Biomineral Interfaces in the Aragonitic Shell of Perna Canaliculus Revealed by Solid-State NMR. *Chem. Mater.* **2013**, *25*, 4595–4602.

(22) Gurinov, A. A.; Mauder, D.; Akcakayiran, D.; Findenegg, G. H.; Shenderovich, I. G. Does Water Affect the Acidity of Surfaces? The Proton-Donating Ability of Silanol and Carboxylic Acid Groups at Mesoporous Silica. *ChemPhysChem* **2012**, *13*, 2282–2285.

(23) Shenderovich, I. G.; Buntkowsky, G.; Schreiber, A.; Gedat, E.; Sharif, S.; Albrecht, J.; Golubev, N. S.; Findenegg, G. H.; Limbach, H.-H. Pyridine- ^{15}N -A Mobile NMR Sensor for Surface Acidity and Surface Defects of Mesoporous Silica. *J. Phys. Chem. B* **2003**, *107*, 11924–11939.

(24) Jayanthi, S.; Kababya, S.; Schmidt, A.; Vega, S. Deuterium MAS NMR and Local Molecular Dynamic Model to Study Adsorption-Desorption Kinetics of a Dipeptide at the Inner Surfaces of SBA-15. *J. Phys. Chem. C* **2016**, *120*, 2797–2806.

(25) Ben Shir, I.; Kababya, S.; Schmidt, A. Binding Specificity of Amino Acids to Amorphous Silica Surfaces: Solid-State NMR of Glycine on SBA-15. *J. Phys. Chem. C* **2012**, *116*, 9691–9702.

(26) Xu, M.; Harris, K. D. M.; Thomas, J. M. Mapping the Evolution of Adsorption of Water in Nanoporous Silica by in Situ Solid-State ^{1}H NMR Spectroscopy. *J. Am. Chem. Soc.* **2008**, *130*, 5880–5882.

(27) Kinney, D. R.; Chuang, I. S.; Maciel, G. E. Water and the Silica Surface As Studied by Variable-Temperature High-Resolution ^{1}H NMR. *J. Am. Chem. Soc.* **1993**, *115*, 6786–6794.

(28) Grünberg, B.; Emmler, T.; Gedat, E.; Shenderovich, I.; Findenegg, G. H.; Limbach, H. H.; Buntkowsky, G. Hydrogen Bonding of Water Confined in Mesoporous Silica MCM-41 and SBA-15 Studied by ^{1}H Solid-State NMR. *Chem. - A Eur. J.* **2004**, *10*, 5689–5696.

(29) Harris, K. D. M.; Xu, M.; Thomas, J. M. Probing the Evolution of Water Clusters during Hydration of the Solid Acid Catalyst H-ZSM-5. *Philos. Mag.* **2009**, *89*, 3001–3012.

(30) Wheatley, P. S.; Chlubná-Eliášová, P.; Greer, H.; Zhou, W.; Seymour, V. R.; Dawson, D. M.; Ashbrook, S. E.; Pinar, A. B.; McCusker, L. B.; Opanasenko, M.; et al. Zeolites with Continuously Tuneable Porosity. *Angew. Chemie Int. Ed.* **2014**, *53*, 13210–13214.

(31) Skorupska, E.; Jeziorna, A.; Paluch, P.; Potrzebowski, M. J. Ibuprofen in Mesopores of Mobil Crystalline Material 41 (MCM-41): A Deeper Understanding. *Mol. Pharm.* **2014**, *11*, 1512–1519.

(32) Azaïs, T.; Tourné-Péteilh, C.; Aussenac, F.; Baccile, N.; Coelho, C.; Devoisselle, J. M.; Babonneau, F. Solid-State NMR Study of Ibuprofen Confined in MCM-41 Material. *Chem. Mater.* **2006**, *18*, 6382–6390.

(33) Werner, M.; Rothermel, N.; Breitzke, H.; Gutmann, T.; Buntkowsky, G. Recent Advances in Solid State NMR of Small Molecules in Confinement. *Isr. J. Chem.* **2014**, *54*, 60–73.

Chapter 4: DNP of $^{13}CO_2$ reacted amine-SBA15

Here, we use DNP to enhance the solid-state NMR studies of APS (aminopropylsilane)-SBA15. The purpose is to interrogate the nature of amine-CO_2 binding via ^{13}C, ^{15}N and ^{29}Si DNP NMR to differentiate between many possible reaction products. The proposed reaction of CO_2 and APS is shown in Scheme 3.1. The DNP enhancement also enables 2D correlation spectra of amine-CO_2 reacted species.

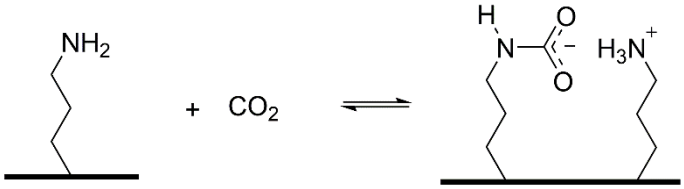

Scheme 4.1 Hypothesized mechanism of CO_2 and APS.

4.1 Overview of DNP

Solid-state NMR is a powerful technique in characterizing structures especially the local coordination environment of amorphous and disordered materials. It is therefore a well-suited tool for mesoporous systems such as amine-SBA15.[1–5] However, solid-state NMR suffers from low sensitivity. Isotopic enrichment is one solution to enhance the signal intensity, but is both costly due to the high cost of the isotopically enriched reagents and can introduce impurities from side products during the labeling process. Dynamic nuclear polarization (DNP) NMR spectroscopy is another promising method to enhance the sensitivity of solid-state NMR by several orders of magnitude. It employs a radical species such as nitroxide to enhance nearby nuclear spins while irradiating the sample with both microwave and radio-frequency pulses to acquire the DNP NMR signal.[2,6] The most common way to introduce the DNP radical agent into

materials is to impregnate the DNP solution. The process includes making a DNP solution, which is made by dissolving a radical in solution and then mixing the DNP solution with the material to be studied. There are several parts in the wetness impregnation that affect the DNP enhancement such as the choice of solvent, the concentration of DNP solution, and the amount of the DNP solution mixing with samples.[2] One technical limit of DNP NMR experiments is that the experiments must be conducted at ≈100 K because of more efficient polarization transfer from electron to nuclei at 100 K. One issue with this scheme, therefore, is that the materials may exhibit different structural details at room temperature compared to 100 K. In this chapter, we show the success of DNP NMR on spectroscopy of the amine-SBA15 and prove that the material can survive at 100 K with DNP solution present.

4.2 Experimental section

NMR experiments: All DNP data were collected in collaboration with Prof. Anne Lesage, Dr. David Gajan, and Dr. Dorothea Wisser, CNRS. DNP was performed on a Bruker 9.4T NMR system (approximately 400 MHz for ^{1}H) and a microwave frequency of 263 GHz. Experiments were performed in 3.2 mm zirconia rotors with an HXY MAS probe. Samples (powders) were combined with a liquid solution of the TEKPol radical species[7] in 1, 1, 2, 2-tetrachloroethane (TCE) (16 mM concentration) using the impregnation technique[8], and samples were loaded in an inert atmosphere glovebox. Experimental DNP data were recorded at a sample temperature of 105 K.

DNP was performed on the $^{13}CO_2$ loaded amine-SBA15. We observed good enhancement of the samples with TEKPol in TCE. There are two enhancement factors (ε) to evaluate whether DNP works. One enhancement factor, ε ($^{1}H/^{13}C$ CP, TCE), is measured by comparing the ^{1}H and ^{13}C

CP intensities of the TCE signals with and without microwave irradiation. These measurements help optimize polarization transfer, including evaluating the concentration of DNP solution, microwave power. Another enhancement factor, ε (^{13}C, carbamate) is measured by comparing the ^{13}C intensities of chemical component in which we are interested. In our case, it is a chemisorbed product species such as carbamate, with and without microwave irradiation. The value represents the enhancement at the surface of the material where this moiety is exposed to the DNP solution, and to evaluate how the DNP radical enhances the material's signal.

Sample preparation: The synthesis of APS-SBA15 and [^{15}N] APS-SBA15 can be found in the previous chapter. The sample was pretreated at 110 °C for 3 h under vacuum in a round-bottom flask on a Schlenk line and cooled to room temperature. The valve of the round-bottom flask was closed, and the flask was transferred to a continuous-flow nitrogen-purged glovebag for packing into glass tubing and subsequently connected to the gas manifold. The sample was then evacuated to 30 mTorr and dosed with 1 atm of $^{13}CO_2$ for 10 h. The glass tubing was flame sealed and then shipped to Lyon, France. The tubing was opened in the glove box. The sample was mixed with the radical which follows the procedure described in the NMR experiments.

4.3 ^{13}C and ^{15}N DNP NMR of APS and [^{15}N] APS

Figure 4.1 shows ^{13}C{^{1}H} DNP CPMAS of $^{13}CO_2$ reacted APS (4 mmol N/g). The resonance at 76 ppm is assigned to TCE which is from the DNP solution. The ^{13}C{^{1}H} DNP CPMAS of $^{13}CO_2$ reacted APS looks no different from the room temperature ^{13}C{^{1}H} CPMAS NMR data (chapter 2), showing that neither the radical nor the low temperature affects the APS and chemisorbed species. Three resonances found at 0-50 ppm are the natural abundance of ^{13}C resonances of APS pendant molecules. The 164 ppm resonance is the chemisorbed product species, which is assigned to an carbamate ion pair.

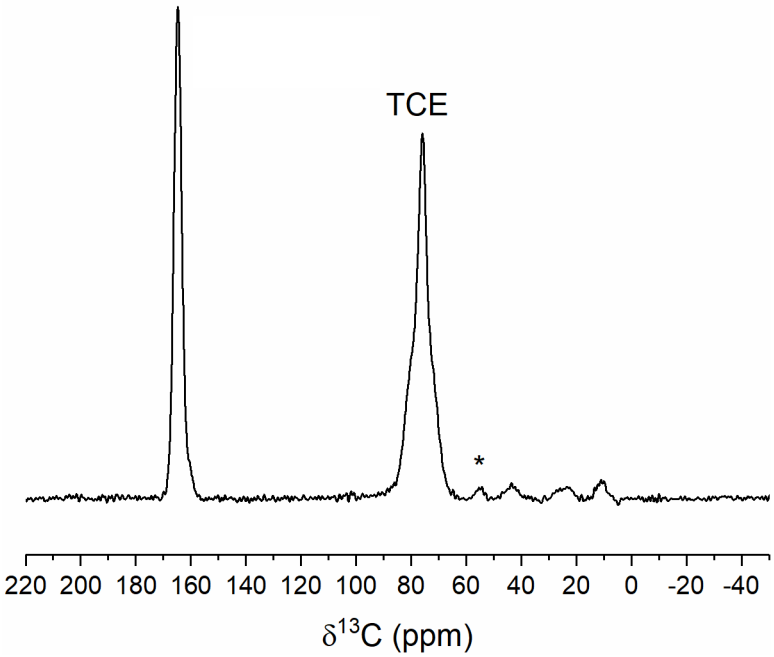

Figure 4.1 $^{13}C\{^{1}H\}$ DNP CPMAS of $^{13}CO_2$ reacted APS-SBA15 (4 mmol N/g) and TCE is solvent from the DNP solution. * denotes a spinning sideband.

The ^{15}N isotope has a natural abundance of 0.365 %.[9] Consequently, its observation without isotopic enrichment is very challenging. We have acquired ^{15}N CPMAS using DNP of the APS sample (at natural abundance). Notably, since we cannot differentiate carbamate and bicarbonate by ^{13}C CPMAS, ^{15}N CPMAS can at least confirm the presence of carbamate. By $^{15}N\{^{1}H\}$ DNP CPMAS, the ^{15}N NMR detection is enhanced. $^{15}N\{^{1}H\}$ DNP CPMAS NMR of $^{13}CO_2$ reacted APS is shown in figure 4.2. The chemisorbed product peak is at 88.3 ppm, and it is assigned to carbamate. The resonance at 33.3 ppm is assigned to a protonated aminopropylsilane which is denoted as “ammonium” in this dissertation (the counter ion of either carbamate or bicarbonate), and the shoulder at 24.3 ppm is unreacted APS.[10] The assignment of ^{15}N resonances can be deferred to chapter 2.

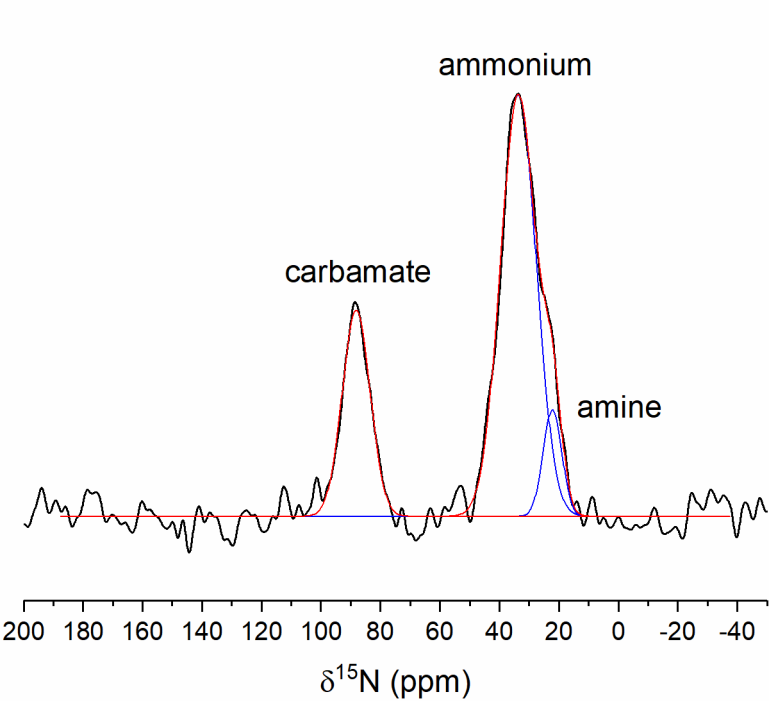

Figure 4.2 $^{15}N\{^{1}H\}$ DNP CPMAS of $^{13}CO_2$ reacted APS (4 mmol N/g). Blue line represents deconvolution, red line represents fitted peaks and black line represents experimental data.

$^{13}C\{^{1}H\}$ DNP CPMAS of [^{15}N] APS-SBA15 is shown is Figure 4.3 for comparison. The ^{13}C resonances at 0-60 ppm are assigned to the natural abundance carbon backbone of pendant APS. Notably, there are four resonances for these carbons instead of three due to the ditethered byproduct of the ^{15}N labeling synthesis whose characterization is given in chapter 2. Interestingly, the sample was not intentionally exposed to $^{13}CO_2$, however there is a small peak located at 164 ppm. This resonance is consistent with carbamate, the chemisorbed product (at natural abundance). It is possible that even without sample activation, the sample is still able to adsorb atmospheric CO_2 leading to this carbamate signal. $^{15}N\{^{1}H\}$ DNP CPMAS of [^{15}N] APS-SBA15 is shown is Figure 4.4. The assignments are identical to those reported in chapter 2. (24 ppm is the APS amine, 32 ppm is ammonium, and 48 ppm is the ditethered byproduct.) Similar

to $^{13}C\{^{1}H\}$ DNP CPMAS (Figure 4.3), there is a small carbamate peak at 88 ppm due to atmospheric CO_2 reacting with the pendant amines.

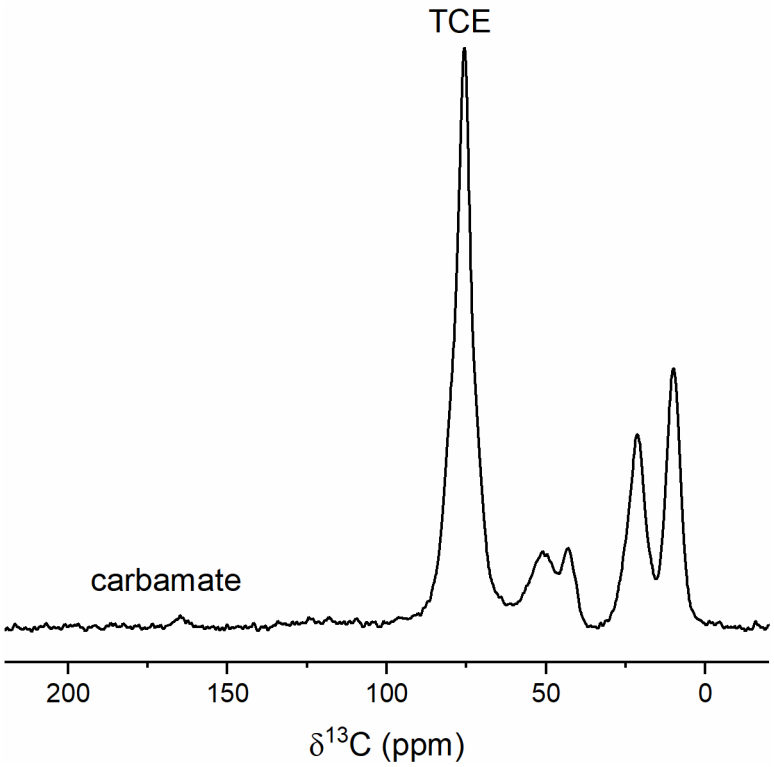

Figure 4.3 $^{13}C\{^{1}H\}$ DNP CPMAS of [^{15}N] APS-SBA15 (1.5 mmol N/g).

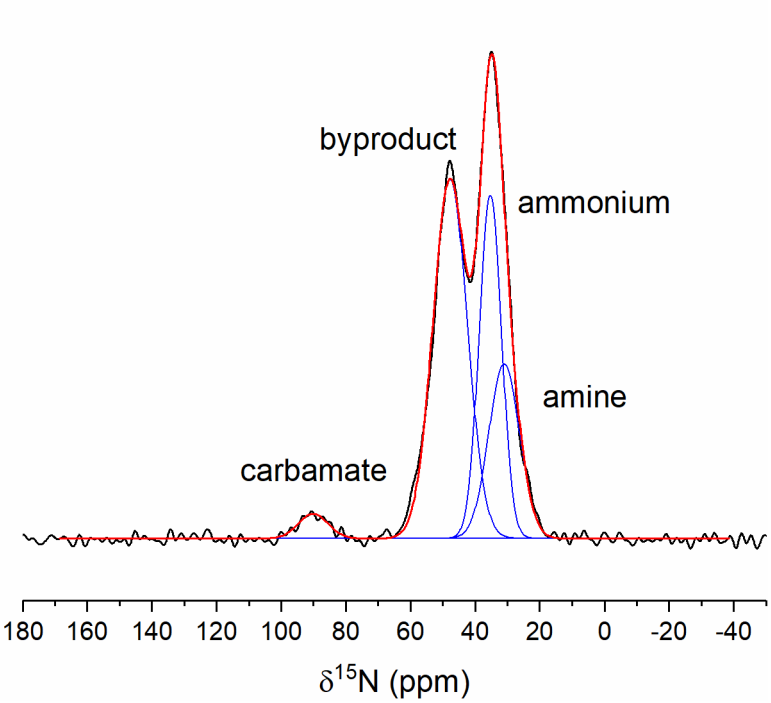

Figure 4.4 $^{15}N\{^{1}H\}$ DNP CPMAS of [^{15}N] APS-SBA15 (1.5 mmol N/g). The blue line represents deconvolution, the red line represents fitted peaks and black line represents experimental data

4.4 DNP HETCOR of APS and [^{15}N] APS

Here, we use DNP to enhance our signal so that it is possible to perform 2-dimensioanl experiments such as HETCOR to provide correlation information between carbon to proton and nitrogen to proton.

Figure 4.5 shows ^{15}N-^{1}H DNP HETCOR of $^{13}CO_2$ reacted APS. The ^{15}N resonance peaked near 32 ppm clearly contains multiple resonances. It can be deconvoluted into two ^{15}N peaks. The shoulder at 24 ppm is assigned to amine (APS) and 32 ppm is assigned to ammonium. The presence of the 24 ppm resonance suggests there are some residual unreacted amines. The ammonium has cross-peaks with two proton environments, ≈ 1 ppm and 9 ppm. The ^{1}H chemical shift of sp^3C methylene and pendant amines are in the range of 1-3 ppm. Therefore, it suggests that ^{15}N ammonium could be coupled to both methylene ^{1}H's and amine ^{1}H's of APS (on its backbone or a neighboring pendant). Another cross-peak at 9 ppm to the ^{1}H from ammonium is consistent with the short-range coupling. This is evidence confirming presence of ammonium (the counter ion to carbamate) which is consistent with the conventional model of carbamate ion pairing. The ^{15}N resonance at 88 ppm is assigned to carbamate, and it has a cross-peak with the same methylene proton. The ^{1}H at a sp^3-carbon could be from the pendant backbone of the chemisorption product or a neighboring APS. Figure 4.6 is a plot overlapping two ^{15}N-^{1}H DNP HETCOR spectra of [^{15}N] APS at two contact times, 250 μs and 1ms. A small ^{15}N resonance at 88 ppm is found corresponding to carbamate ^{15}N from amines adventitiously reacting with atmospheric CO_2. The ^{15}N carbamate resonance has cross-peaks with two distinct protons at different contact times. Carbamate is correlated with ^{1}H at 4.8 ppm at the shorter contact time, which we deposit is the directly-bonded proton of carbamate. At the longer contact time, the experiment allows increased ^{1}H-^{1}H spin diffusion, so the proton signal of carbamate becomes

less resolvable in the proton bath including the proton of methylene, amine, and ammonium. Here, since we observe ^{15}N of ammonium and carbamate directly, there are few ambiguities assigning protons of carbamate and proton of ammonium by ^{15}N-^{1}H DNP HETCOR.

^{13}C-^{1}H DNP HETCOR of $^{13}CO_2$ reacted APS (4 mmol N/g) is shown in Figure 4.7. The ^{13}C resonance at 164 ppm is assigned to carbamate from $^{13}CO_2$ chemisorption, and three resonances at 0-40 ppm are assigned to the carbon backbone (natural abundance) of APS. The resonance at 70 ppm is from the DNP solvent, TCE. The ^{13}C resonance of carbamate has a strong cross-peak with the proton at 2 ppm with a long "tail" that extends up to 12 ppm. ^{1}H at 2 ppm is in the range of methylene and amine protons. The spectrum is consistent with the previous finding (in Figure 4.7) that carbamate couples to methylene and amines in the ^{15}N-^{1}H DNP HETCOR. The long tail of the cross-peak at 164 ppm is interesting because a similar correlation was not found for ^{15}N-^{1}H DNP HETCOR. It is possible that the proton of carbamate (at 4.8 ppm for ^{1}H) and proton of nearby ammonium in the ion pair (9 ppm) are both present resulting in a long tail. Another possibility is that carbamate-bearing pendant bends to the surface and couples to the surface hydroxides that are present on silica (^{1}H of $\approx$ 5.5 ppm). The hydrogen bonding between carbamate, surface and water molecules on the surface could lead to similar chemical shifts, such that the protons overlap each other and cannot be resolved.

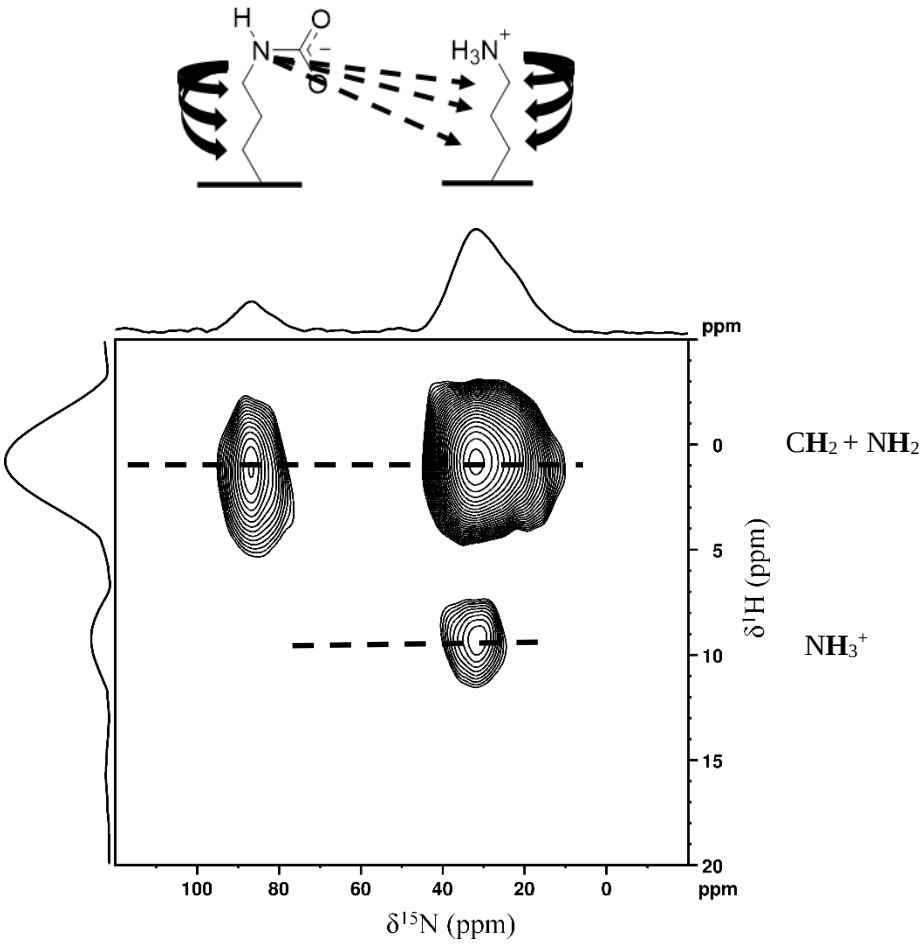

Figure 4.5 ^{15}N-^{1}H DNP HETCOR of $^{13}CO_2$ reacted APS (4 mmol N/g). Contact time is 1 ms. Dotted line at ≈1 ppm corresponds to ^{1}H's of C**H**$_2$, N**H**$_2$ or both, and dotted line at 9 ppm corresponds to ^{1}H's of N**H**$_3^+$.

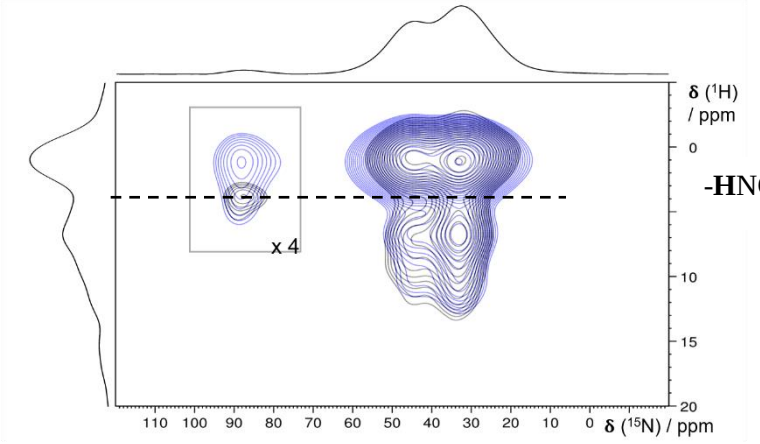

Figure 4.6 ^{15}N-^{1}H DNP HETCOR of **[^{15}N]** APS (1.5 mmol N/g). Black represents 250 µs of contact time and blue represents 1 ms of contact time. Dotted line at 4 ppm corresponds -**H**NCOO$^-$.

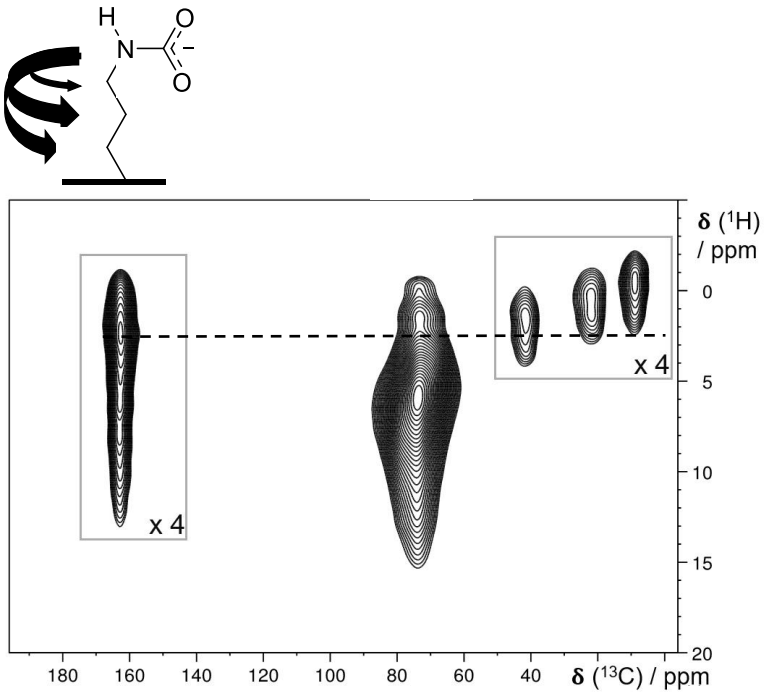

Figure 4.7 $^{13}C\{^{1}H\}$ DNP HETCOR of $^{13}CO_2$ reacted APS (4 mmol). The contact time is 1 ms. Dotted line is a guide to the eye.

4.5 $^{29}Si\{^{13}C\}$ DNP REDOR of APS using ^{29}Si-^{1}H HETCOR

The enhancement of DNP allows us to perform 2-dimentional experiments that would be too time consuming with conventional NMR. To understand the interaction between $^{13}CO_2$ reacted APS and the silica surface, the Lyon group performed the proton edited $^{29}Si\{^{13}C\}$ REDOR experiments.[11] The REDOR spectra are recorded as a series of 2D ^{29}Si-^{1}H HETCOR spectra, where each spectrum corresponds to either a S_0 (without dephasing pulses) or S (with ^{13}C

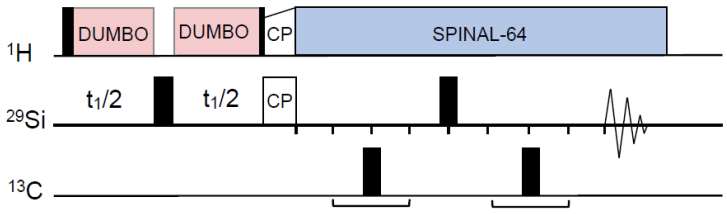

Figure 4.8 proton edited $^{29}Si\{^{13}C\}$ REDOR sequence.

dephasing pulses). Slices are then extracted along the proton dimension to follow the dephasing effect of a given carbon resonance. The sequence is depicted in Figure 4.8.

The ^{29}Si-^{1}H DNP HETCOR of $^{13}CO_2$ reacted APS is shown in Figure 4.9. The spectrum shows two ^{29}Si resonances at ≈ -100 and ≈ -68 ppm, and the chemical shift is consistent with Q^3 (Si $(OSi)_3(OH)$) and T^3 ($RSi(OSi)_3$, R being the alkyl chain) correspondingly.[12,13] Q^3 (Si $(OSi)_3(OH)$) couples to two protons at 2.5 ppm and 6.8 ppm. The ^{1}H at 2.5 ppm is the surface hydroxide[14] and 6.8 ppm resonance is a surface hydroxide that is hydrogen bonded to other species such as H_2O or APS.[13,15] Here, we examine the surface hydroxide of Q^3 sites to see if there is interaction between surface hydroxide and carbamate. The slices which are corresponding to the hydroxide at 2.5 ppm are extracted to follow selective dephasing of ^{13}C carbamate (164 ppm). If there is no dipolar interaction of carbamate and surface hydroxide, then there would be no intensity difference with or without ^{13}C dephasing pulses. The results are shown in Figure 4.10. At a shorter dephasing time of 0.16 ms, the two spectra look identical with error on the order of noise. After 0.16 ms, each spectrum begins to show differences when compared to the spectra with ^{13}C dephasing pulses. This difference arises if carbamate dipolar coupled with the surface hydroxide. If carbamate experiences such surface-mediated dipole-dipole coupling, we posit that carbamate is oriented (or tilted) toward the surface. Furthermore, the long tail in the ^{13}C-^{1}H HETCOR for the 164 ppm resonance reflects a range of dipolar coupling – not discrete 2-spin interactions.

.

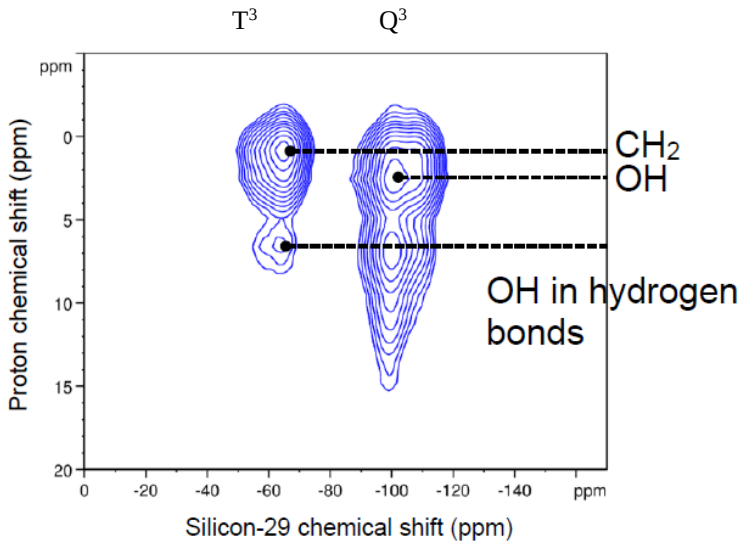

Figure 4.9 ^{29}Si-^{1}H DNP HETCOR of $^{13}CO_2$ reacted APS. Dotted line at 1 ppm represents C**H**$_2$, 2.5 ppm represents O**H**, and 6.8 ppm represents O**H** in hydrogen bonds.

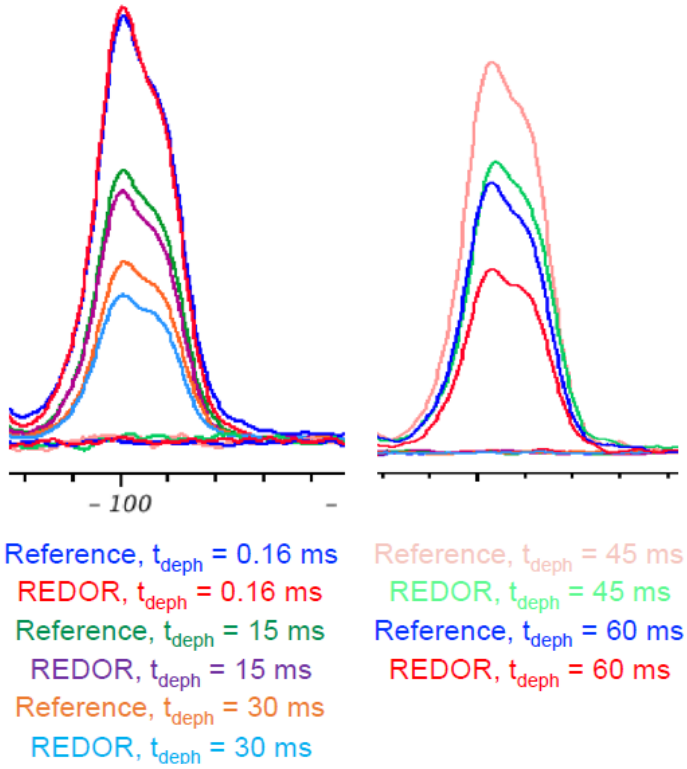

Figure 4.10 ^{29}Si slices in ^{29}Si-^{1}H DNP HETCOR of $^{13}CO_2$ reacted APS are extracted at δ^{1}H 2.5 ppm with ^{13}C dephasing pulses and without dephasing pulses. Reference represents without ^{13}C dephasing pulse and REDOR represents with ^{13}C dephasing pulse.

4.6 Conclusion

We show that DNP was successfully performed on the amine-SBA15. Both ^{13}C and ^{15}N could be observed at natural abundance. The chemisorbed species, carbamate, was found in $^{13}C\{^{1}H\}$ DNP CPMAS and $^{15}N\{^{1}H\}$ of $^{13}CO_2$ reacted APS. However, the 1D spectra were not enough to fully understand the system. The DNP enhancement enabled 2D HETCOR spectra to be recorded. The combination of ^{15}N-^{1}H DNP HETCOR and ^{13}C-^{1}H DNP HETCOR gave a picture of dipole-dipole interactions between APS and carbamate. Carbamate and ammonium (the counter ion of carbamate), show strong coupling to methylene 1H's and this interaction could be from the pendant, neighboring APS, or both. We report the -**H**NCOO- of carbamate is 4.8 ppm and N**H**$_3^+$ of ammonium is 9 ppm by ^{15}N-^{1}H DNP HETCOR. The long "tail" found in ^{13}C-^{1}H DNP of carbamate resonance suggests there is has hydrogen bonding to the surface silanol groups. Furthermore, we use slice-selective ^{29}Si-^{1}H HETCOR to designate resonances for targeted ^{13}C REDOR dephasing by $^{29}Si\{^{13}C\}$ DNP REDOR of $^{13}CO_2$ reacted APS. The ^{29}Si spectra show differences between S_0 (without dephasing pulses on the ^{13}C carbamate signal) and S (with ^{13}C dephasing pulse on carbamate) which suggests that the carbamate experiences a dipole-dipole interactions to the surface hydroxide.

References (Chapter 4)

(1) Eedugurala, N.; Wang, Z.; Chaudhary, U.; Nelson, N.; Kandel, K.; Kobayashi, T.; Slowing, I. I.; Pruski, M.; Sadow, A. D. Mesoporous Silica-Supported Amidozirconium-Catalyzed Carbonyl Hydroboration. *ACS Catal.* **2015**, *5*, 7399–7414.

(2) Rossini, A. J.; Zagdoun, A.; Lelli, M.; Lesage, A.; Cop, C.; Emsley, L. Dynamic Nuclear Polarization Surface Enhanced NMR Spectroscopy. *Acc. Chem. Res.* **2013**, *46*, 1942–1951.

(3) Lelli, M.; Gajan, D.; Lesage, A.; Caporini, M. A.; Vitzthum, V.; Miéville, P.; Héroguel, F.; Rascón, F.; Roussey, A.; Thieuleux, C.; et al. Fast Characterization of Functionalized Silica Materials by Silicon-29 Surface-Enhanced NMR Spectroscopy Using Dynamic Nuclear Polarization. *J. Am. Chem. Soc.* **2011**, *133*, 2104–2107.

(4) Lafon, O.; Thankamony, A. S. L.; Kobayashi, T.; Carnevale, D.; Slowing, I. I.; Kandel, K.; Amoureux, J.; Pruski, M. Mesoporous Silica Nanoparticles Loaded with Surfactants : Low Temperature Magic-Angle Spinning ^{13}C and ^{29}Si NMR Enhanced by Dynamic Nuclear Polarization. *J. Phys. Chem. C* **2013**, *117*, 1375–1382.

(5) Lafon, O.; Rosay, M.; Aussenac, F.; Lu, X.; Trébosc, J.; Cristini, O.; Kinowski, C.; Touati, N.; Vezin, H.; Amoureux, J. P. Beyond the Silica Surface by Direct Silicon-29 Dynamic Nuclear Polarization. *Angew. Chemie - Int. Ed.* **2011**, *50*, 8367–8370.

(6) Maly, T.; Debelouchina, G. T.; Bajaj, V. S.; Hu, K.-N.; Joo, C.-G.; Mak-Jurkauskas, M. L.; Sirigiri, J. R.; van der Wel, P. C. a; Herzfeld, J.; Temkin, R. J.; et al. Dynamic Nuclear Polarization at High Magnetic Fields. *J. Chem. Phys.* **2008**, *128*, 052211–0552219.

(7) Zagdoun, A.; Casano, G.; Ouari, O.; Schwarzwälder, M.; Rossini, A. J.; Aussenac, F.; Yulikov, M.; Jeschke, G.; Coperet, C.; Lesage, A.; et al. Large Molecular Weight Nitroxide Biradicals Providing Effi-Cient Dynamic Nuclear Polarization at Temperatures up to 200 K. *J. Am. Chem. Soc.* **2013**, *135*, 12790–12797.

(8) Zagdoun, A.; Rossini, A. J.; Gajan, D.; Bourdolle, A.; Ouari, O.; Rosay, M.; Maas, W. E.; Tordo, P.; Lelli, M.; Emsley, L.; et al. Non-Aqueous Solvents for DNP Surface Enhanced NMR Spectroscopy. *Chem. Commun.* **2012**, *48*, 654–656.

(9) Martin, G.J., Martin, M.L., Gouesnard, J.-P. *^{15}N-NMR Spectroscopy*; Springer-Verlag: Berlin, 1981.

(10) Perinu, C.; Saramakoon, G.; Arstad, B.; Jens, K.-J. Application of ^{15}N-NMR Spectroscopy to Analysis of Amine Based CO_2 Capture Solvents. *Energy Procedia* **2014**, *63*, 1144–1150.

(11) Sangodkar, R. P.; Smith, B. J.; Gajan, D.; Rossini, A. J.; Roberts, L. R.; Funkhouser, G. P.; Lesage, A.; Emsley, L.; Chmelka, B. F. Influences of Dilute Organic Adsorbates on the Hydration of Low-Surface-Area Silicates. *J. Am. Chem. Soc.* **2015**, *137*, 8096–8112.

(12) Rassy, H. El; Pierre, A. C. NMR and IR Spectroscopy of Silica Aerogels with Different Hydrophobic Characteristics.

(13) Mafra, L.; Cendak, T.; Schneider, S.; Wiper, P. V.; Pires, J.; Gomes, J. R. B.; Pinto, M. L. Structure of Chemisorbed CO_2 Species in Amine-Functionalized Mesoporous Silicas Studied by Solid-State NMR and Computer Modeling. *J. Am. Chem. Soc.* **2017**, *139*, 389–408.

(14) Trébosc, J.; Wiench, J. W.; Huh, S.; Lin, V. S.-Y.; Pruski, M. Solid-State NMR Study of MCM-41-Type Mesoporous Silica Nanoparticles. *J. Am. Chem. Soc.* **2005**, *127*, 3057–3068.

(15) Hung, C.-T.; Yang, C.-F.; Lin, J.-S.; Huang, S.-J.; Chang, Y.-C.; Liu, S.-B. Capture of Carbon Dioxide by Polyamine-Immobilized Mesostructured Silica: A Solid-State NMR Study. *Micropouous mesoporous Mater.* **2017**, *238*, 2–13.

Chapter 5: Conclusions and future directions

5.1 Conclusions

We have interrogated the interaction of CO_2 and solid amine sorbents, primarily through employing solid-state NMR to study these materials. Multiple chemisorbed products species were found in spectra including ^{13}C, and ^{15}N CPMAS. However, the chemical shift assignment alone was not enough to determine the possible chemisorbed product species. More advanced NMR techniques were therefore used to confirm the formation of carbamic acid, carbamate ion pairs, and bicarbonate in the primary amine, aminopropylsilane (APS) reacting with $^{13}CO_2$ under "dry" condition (not intentionally adding water) : (1) $^{15}N\{^{13}C\}$REDOR of APS allows us to determine the strength of the heteronuclear dipole-dipole interaction of chemisorbed product species, from which we were able to extract the distance information of both the directly-bonded C-N pair carbamate (at 1.42 Å) and the more distant C-N interaction between the ^{13}C on carbamate and its counterion, ammonium ^{15}N (3.13 Å). Furthermore, some of the reduced intensity of the $^{13}C\{^{15}N\}$ REDOR curve (the lack of a buildup to 100%) is consistent with the presence of bicarbonate as a side-product in the chemisorption of CO_2 on APS. (2) Monitoring the product intensity over time suggests carbamic acid overlaps with carbamate in ^{15}N spectrum, and carbamic acid, being less stable, converts to amine as the sample ages. (3) We show DNP NMR is able to resolve structures of in the mesoporous surfaces of the solid amine sorbents and with good enhancement. By using the 2D HETCOR (via DNP) including ^{13}C-^{1}H, ^{15}N-^{1}H, and ^{29}Si-^{1}H, these data elucidate interactions of the carbamate ion pair and SBA15 surface. The coupling in ^{13}C-^{1}H and ^{29}Si-^{1}H HETCOR suggest the carbamate is coupled to the surface through hydrogen bonding to Si-OH.

Under humid (or water-dampened) conditions of solid amine sorbents reacting with $^{13}CO_2$, we found bicarbonates are able to be formed in all three types of amine: primary, secondary, and tertiary. Water not only facilitates the reaction of amines and CO_2 to form bicarbonate, but also induces dynamic motion of bicarbonate leading to very inefficient detection by CPMAS NMR, the most ubiquitous solid-state NMR technique used to detect ^{13}C. In order to test the hypothesis of dynamics interfering with the NMR experiments at room temperature, the materials were cooled down to temperatures as low as 100K. The single room temperature bicarbonate signal in the tertiary amine, DMAPS (where bicarbonate is the *only* chemisorption product), turns into two bicarbonate signals, at 162 and 168 ppm,at these low temperatures, indicating two magnetically- and chemically-inequivalent bicarbonate species. By using D_2O in place of water to wet the solid-amine sorbent prior to $^{13}CO_2$ exposure to reduce the strong homonuclear interaction from ^1H in H_2O, we were able to assign the bicarbonate signals by ^{13}C-^1H HETCOR: One bicarbonate (^{13}C 168 ppm) is surrounded by water which does not couple to the surface, and the other bicarbonate (^{13}C 162 ppm) is coupled to the surface water. Both are in close enough proximity to couple to the protons on the sp^3 carbons of the pendant groups.

5.2 Future directions

The ultimate goal for studying the solid-amine sorbents is to find better materials to capture CO_2. We chose a series of amines (APS (1°), MAPS (2°), and DMAPS (3°)) as model compounds to probe the interaction of CO_2 and solid amine sorbents. Insights from NMR will allow researchers to develop practical and cost-effective solid amine sorbents materials, meaning higher CO_2 uptake such as amine polymers, poly(ethyleneimine) (PEI), with lower energy costs for post-capture regeneration. For example, the finding of bicarbonate enters a relatively recent debate about its existence in these solid-amine sorbents, because it is believed to require higher energy

to regenerate the materials. In addition, the new finding to test for the presence of bicarbonate by using Bloch decay NMR is critical for the entire community that characterizes these materials.

One practical aspect is to study experimental conditions that mimics real flue gas conditions such as humidity, and mixed gases (N_2, NO_2, SO_2). The study could be explored in several ways: (1) An investigation to see if acid gases such as NO_2 and SO_2 would affect the structures of solid amine sorbents. To characterize the structures of solid amine sorbents after acid gas exposure to see if there are any changes in dry and humid condition. (2) Load $^{13}CO_2$ to examine if the chemisorbed products are the same without acid gas exposure. And more importantly, are the products still reversible after acid gases exposure? (3) Load mixed-gas on the solid-amine sorbent and characterize the chemisorbed products. Is CO_2 of the flue gas the most favored gas to be adsorbed on solid-state amine sorbents, and are the $^{13}CO_2$ chemisorbed product species the same when other acid gases present such as N_2+CO_2, and H_2O vapor+CO_2+NO_2? (4) Does the experimental condition that mimics the flue gas affect the CO_2 adsorption efficiency, and how does it affect? Is the changed efficiency from structural changes of solid amines or from unexpected chemistry happen in the system?

Numerous questions can be derived from combinations of solid supports, different amines infiltrating the high surface area materials, different conditions of temperature and humidity under which the gas is captured (or released), and whether flue gases need some level of pre-treatment before exposure to the sorbent. Solid-state NMR provides a “window” into many of these processes, as the materials are engineered to assist with CO_2 reduction.

Curriculum Vitae

Chia-Hsin Chen

PhD Candidate in Chemistry
Email: chia-hsin@wustl.edu
Phone (Cell): (+1) 314-9525910
Phone (Lab): (+1) 314-9355031

Education

Ph.D. Candidate Chemistry, Washington University in St. Louis (WUSTL)	2013-present
M.S. Chemistry, National Central University, Taiwan	2010-2012
B.S. Applied Chemistry, National Chi Nan University, Taiwan	2006-2010

Research Experiences

Washington University in St. Louis, Advisor: Sophia E. Hayes — 2013-present
Graduate research: Solid-state NMR on solid amine modified SBA15

- Using solid-state NMR to characterize the structure of disordered materials used for carbon capture including metal-organic framework systems and silica-supported mesoporous amines. These studies inform the better synthesis and design for CO_2-capture materials to help remediate the effects of CO_2 on the environment.

National Central University, Taiwan. Advisor: Bor-Chen Chang — 2010-2012
Graduate research: Unknown bands observed in the 266 nm photolysis of iodomethanes

- Using Nd-Yag laser and dye laser to study the photolysis of iodomethanes. Such studies develop an understanding of how halomethane affects the ozone layer.

National Chi Nan University, Taiwan. Advisor: Li-Hsin Chan — 2008-2010
Undergraduate independent research: Organic light emitting diode (OLED)

- Synthesis and characterization of high-quantum-yield pyrrole-based fluorophore. The study is to explore time and cost-efficient method of making OLED.

Honors and Awards

59th ENC student travel award, Orlando FL	2018
Taiwan Ministry of Education/Washington University in St. Louis Fellowship	2013-2017
The Best Student Poster Award in the 2011 Annual Meeting of Chinese Chemical Society, Taiwan	2011

Presentations

Oral presentations

ACS Midwest Regional Meeting, Ames IA	2018
Missouri Inorganic Day	2017

Poster presentations

Rocky Mountain Conference on Magnetic Resonance (RMC), UT	2018
Experimental Nuclear Magnetic Resonance Conference (ENC), Orlando FL	2018
Chicago Area NMR Discussion Group, Chicago IL	2017
Experimental Nuclear Magnetic Resonance Conference (ENC), Pacific Grove CA	2017
Chicago Area NMR Discussion Group, Milwaukee WI	2016
Rocky Mountain Conference on Magnetic Resonance (RMC), CO	2016

Publications

(1) **Chen, C.-H.**; Shimon, D.; Lee, J. J.; Mentink-Vigier, F.; Hung, I.; Sievers, C.; Jones, C. W.; Hayes, S. E. The "Missing" Bicarbonate in CO_2 Chemisorption Reactions on Solid Amine Sorbents. *J. Am. Chem. Soc.* **2018**, *140*, 8648–8651.

(2) **Chen, C.-H.**; Shimon, D.; Lee, J. J.; Didas, S. A.; Mehta, A. K.; Sievers, C.; Jones, C. W.; Hayes, S. E. Spectroscopic Characterization of Adsorbed $^{13}CO_2$ on 3-Aminopropylsilyl-Modified SBA15 Mesoporous Silica. *Environ. Sci. Technol.* **2017**, 6553–6559.

(3) Shimon, D.; **Chen, C.-H**.; Lee, J. J.; Didas, S. A.; Sievers, C.; Jones, C. W.; Hayes, S. E. ^{15}N Solid State NMR Spectroscopic Study of Surface Amine Groups for Carbon Capture: 3-Aminopropylsilyl Grafted to SBA-15 Mesoporous Silica. *Environ. Sci. Technol.* **2018**, *52*, 1488–1495.

(4) Lee, J. J.; Yoo, C.-J.; **Chen, C.-H.**; Hayes, S. E.; Sievers, C.; Jones, C. W. Silica-Supported Sterically Hindered Amines for CO_2 Capture. *Langmuir* **2018**, *34*, 12279–12292.

(5) Foo, G. S.; Lee, J. J.; **Chen, C.-H.**; Hayes, S. E.; Sievers, C.; Jones, C. W. Elucidation of Surface Species through in Situ FTIR Spectroscopy of Carbon Dioxide Adsorption on Amine-Grafted SBA-15. *ChemSusChem* **2017**, *10*, 266–276.

(6) Lee, J. J.; **Chen, C.-H.**; Shimon, D.; Hayes, S. E.; Sievers, C.; Jones, C. W. Effect of Humidity on the CO_2 Adsorption of Tertiary Amine Grafted SBA-15. *J. Phys. Chem. C* **2017**, *121*, 23480–23487.